The competing effects of sulfide saturation versus degassing on the behavior of the chalcophile elements during the differentiation of hydrous melts

Citation	Jenner, F. E., Hauri, E. H., Bullock, E. S., König, S., Arculus, R. J., Mavrogenes, J. A., ... & Goddard, C. (2015). The Competing Effects of Sulfide Saturation versus Degassing on the Behavior of the Chalcophile Elements during the differentiation of hydrous melts. Geochemistry, Geophysics, Geosystems, 16(5), 1490-1507. doi:10.1002/2014GC005670
DOI	10.1002/2014GC005670
Publisher	John Wiley & Sons Ltd.
Version	Version of Record
Terms of Use	http://cdss.library.oregonstate.edu/sa-termsofuse

AGU PUBLICATIONS

Geochemistry, Geophysics, Geosystems

RESEARCH ARTICLE
10.1002/2014GC005670

Special Section:
Assessing Magmatic, Neovolcanic, Hydrothermal, and Biological Processes Along Intra-Oceanic Arcs and Back-Arcs

The competing effects of sulfide saturation versus degassing on the behavior of the chalcophile elements during the differentiation of hydrous melts

Frances E. Jenner[1,2], Erik H. Hauri[2], Emma S. Bullock[3], Stephan König[4], Richard J. Arculus[5], John A. Mavrogenes[5], Nicole Mikkelson[5], and Charlotte Goddard[6]

[1]Department of Environment, Earth and Ecosystems, Open University, Milton Keynes, UK, [2]Department of Terrestrial Magnetism, Carnegie Institution of Washington, Washington, District of Columbia, USA, [3]Department of Mineral Sciences, National Museum of Natural History, Smithsonian Institution, Washington, District of Columbia, USA, [4]Isotopengeochemie, Universität Tübingen, Tübingen, Germany, [5]Research School of Earth Sciences, Australian National University, Canberra, Australian Capital Territory, Australia, [6]Department of Fisheries and Wildlife, Oregon State University, Corvallis, Oregon, USA

Abstract There is a lack of consensus regarding the roles of sulfide saturation versus volatile degassing on the partitioning of Cu and Ag during differentiation and eruption of convergent margin magmas. Because of their oxidized character, volatile-rich magmas from the Eastern Manus Back-arc Basin (EMBB) only reach sulfide saturation following magnetite-driven reduction of the melt: the so-called "magnetite crisis." If sulfide saturation typically precedes volatile saturation, the magnetite crisis will limit the proportion of Cu and Ag that can partition from the melt into an exsolving volatile-rich phase, which may contribute to the sporadic occurrence of magmatic-hydrothermal ore deposits at convergent margins. However, it is unclear whether the magnetite crisis is a common or rare event during differentiation of volatile-rich magmas. We report major and trace element data for submarine volcanic glasses from the Tonga arc-proximal Valu Fa Ridge (VFR; SW Pacific). Cu-Se-Ag systematics of samples erupting at the southern VFR suggest magnetite fractionation-triggered sulfide saturation. The similarity in chalcophile element systematics of the southern VFR and EMBB samples is unlikely to be coincidental, and may indicate that the magnetite crisis is a common event during differentiation of hydrous melts. However, unlike many convergent margin magmas, it is unlikely that the evolving VFR and EMBB were saturated in a S-bearing volatile phase prior to magnetite fractionation. Hence, the metal-depleting magnetite crisis may be restricted to back-arc basin magmas that do not degas volatiles prior to magnetite fractionation and potentially convergent margin magmas fractionating at high pressures in the continental crust.

Key Points:
- Magmas erupting in the Lau Basin record magnetite-triggered sulfide saturation
- We evaluate the roles of sulfides versus degassing on melt composition
- We evaluate potential causes of the sporadic occurrence of ore deposits

Supporting Information:
- Supporting Information S1
- Tables S1-S6

Correspondence to:
F. E. Jenner,
frances.jenner@open.ac.uk

Citation:
Jenner, F. E., E. H. Hauri, E. S. Bullock, S. König, R. J. Arculus, J. A. Mavrogenes, N. Mikkelson, and C. Goddard (2015), The competing effects of sulfide saturation versus degassing on the behavior of the chalcophile elements during the differentiation of hydrous melts, *Geochem. Geophys. Geosyst.*, *16*, 1490–1507, doi:10.1002/2014GC005670.

Received 26 NOV 2014
Accepted 24 APR 2015
Accepted article online 30 APR 2015
Published online 26 MAY 2015

1. Introduction

Magmatic-hydrothermal ore deposits (e.g., porphyry and epithermal) are globally and spatially associated with convergent margins [e.g., *Hedenquist and Lowenstern*, 1994; *Richards*, 2011; *Sillitoe*, 2010] and are typically considered to be sourced from magma chambers located at depths of 4–10 km in the crust [e.g., *Cooke et al*., 2014, and references therein]. The extent to which this association is related to source characteristics versus crustal processes remains contentious. Proponents of the enriched source hypotheses have argued for subduction-derived metal enrichment of the wedge, or inheritance from the subcontinental lithospheric mantle [e.g., *Mungall*, 2002; *Tan et al*., 2012, and references therein]. Other studies have demonstrated that primitive magmas erupting at convergent margins need not be enriched in metals relative to MORB magmas [*Cline and Bodnar*, 1991; *Hamlyn et al*., 1985; *Jenner et al*., 2010; *Lee et al*., 2012]. Instead, they attribute the association to processes taking place in the crust [*Candela and Holland*, 1986; *Hedenquist and Lowenstern*, 1994; *Jenner et al*., 2010; *Richards*, 2003; *Wilkinson*, 2013].

There are three main stages considered essential to the formation of magmatic-hydrothermal ore deposits: (1) crystallization of melts in upper crustal magma chambers; (2) exsolution of aqueous fluids; and (3) post-exsolution modification of the aqueous fluid and precipitation of ore minerals [e.g., *Audétat et al*., 2008; *Blundy et al*., 2015; *Hedenquist and Lowenstern*, 1994; *Richards*, 2003; *Sillitoe*, 2010; *Wilkinson*, 2013]. Studies

of the magmatic-hydrothermal ore deposits give an unrivaled view of the role of the post-exsolution history of magma-derived aqueous fluids in ore formation [e.g., *Bodnar et al*., 2014]. Whereas in situ studies of volcanic glasses erupted on the seafloor at convergent margins and mineral-hosted melt inclusions give an unique opportunity (e.g., minimal crustal contamination and secondary alteration) to assess the role of melt composition and magma chamber processes in determining whether a given batch of magma is likely to fuel the formation of a magmatic-hydrothermal ore deposit, which is the focus of this study.

In situ analysis of olivine-hosted melt inclusions from a global selection of convergent margins show a range in $Fe^{3+}/\Sigma Fe$ up to 0.32 (highest value from Augustine, Aleutians), which are considerably higher than MORB at 0.16 ± 0.01 [*Cottrell and Kelley*, 2011; *Kelley and Cottrell*, 2009]. At such high fO_2, the content of S required to reach sulfide saturation can be up to 1.4 wt % [*Jugo*, 2009]. Analyses of melt inclusions show that even convergent margin magmas with high $Fe^{3+}/\Sigma Fe$, such as those from Augustine, have $<$6000 ppm S [e.g., *Kelley and Cottrell*, 2009; *Zimmer et al*., 2010]. Hence, unlike MORB, which show early and sustained removal of Fe-Ni sulfide liquid [e.g., *Czamanske and Moore*, 1977; *Mathez*, 1976; *Patten et al*., 2013], convergent margin magmas are likely to remain sulfide undersaturated during initial differentiation, allowing Cu, Ag, and Au contents to build up in the melt to levels considerably higher than MORB [*Jenner et al*., 2010; *Lee et al*., 2012; *Park et al*., 2015].

It has been suggested that the fractionation of magnetite from evolving convergent margin magmas is likely to result in a drop in the fO_2 of the evolving melt, because of the extremely high $Fe^{3+}/\Sigma Fe$ of magnetite (0.67) compared to typical convergent margin magmas [*Jenner et al*., 2010; *Sun et al*., 2004]. Volatile-rich samples from the arc-proximal Eastern Manus Back-arc Basin (EMBB), located in the western Pacific show an initial increase in $Fe^{3+}/\Sigma Fe$ with increasing SiO_2 up to 60 wt %, after which there is a drop in $Fe^{3+}/\Sigma Fe$ and thereafter stabilization at relatively constant $Fe^{3+}/\Sigma Fe$ with further increases in SiO_2 [see *Jenner et al*., 2010, Figure 11]. Because of the redox exchange equilibria between Fe and S and the stoichiometry of the reaction [see *Jenner et al*., 2010], the modest change in $Fe^{3+}/\Sigma Fe$ (0.3 to 0.2) resulting from magnetite removal is sufficient to drive the dissolved S in the melt from mostly SO_4^{2-} to mostly S^{2-} (fraction of total S as SO_4^{2-} drops from 0.9 to 0.25). In addition to the decrease in S solubility of the melt with decreasing in ΣFe [*Mavrogenes and O'Neill*, 1999], fractional crystallization of magnetite is likely to trigger sulfide saturation. This feature of magmatic evolution, affectionately termed the "magnetite crisis" [*Jenner et al*., 2010], is exemplified by the EMBB suite, which show a sudden plummet in the contents of chalcophile elements such as Cu, Se, Ag, and Au and chalcophile element ratios such as Cu/Se and Ag/Se after the appearance of magnetite on the liquidus. Magnetite-triggered sulfide saturation has subsequently been used to explain the change in partitioning behavior of Cu, Au, and Pd following the appearance of magnetite on the liquidus during differentiation of rear arc magmas erupting in the NE Lau Basin, SW Pacific [*Park et al*., 2015].

The common occurrence of magnetite on the liquidus of evolving convergent margin magmas [*Arculus*, 2004; *Sisson and Grove*, 1993; *Zimmer et al*., 2010] suggests the magnetite crisis could be a common event during differentiation of hydrous melts. A drop in fO_2 resulting from magnetite fractionation would seem contrary to the long-standing observation that Fe-Ti oxide saturated arc magmas typically show near-constant fO_2 with decreasing equilibrium temperature [*Carmichael*, 1991, 1967; *Hildreth*, 1983]. Indeed, the EMBB magmas in which the magnetite crisis was first observed show only a modest drop ($Fe^{3+}/\Sigma Fe$ of 0.3–0.2) at the onset of magnetite crystallization, and a nearly constant ratio thereafter [see *Jenner et al*., 2010, Figure 11]. These systematics may imply pure end-member magnetite is quickly replaced on the liquidus by magnetite (Fe_3O_4)-ulvöspinel (Fe_2TiO_4) solid solution [*Bosi et al*., 2009], thereby limiting further decreases in $Fe^{3+}/\Sigma Fe$ of the melt. Additionally, because the proposed magnetite crisis event coincides with the dearth in $\sim$60–65 wt % SiO_2 erupted magma compositions [e.g., *Hildreth*, 1983; *Melekhova et al*., 2013], it is perhaps unsurprising that the "event" leaves little evidence other than an abrupt change in chalcophile element systematics resulting from magnetite-triggered sulfide saturation. However, few Cu, Se, and Ag analyses are available in the literature, making it difficult to assess whether the magnetite crisis is taking place in regions other than the EMBB and the NE Lau Basin. Regardless of the cause, if sulfide saturation is a common event during differentiation of convergent margin magmas, the "trapping" of chalcophile elements in sulfides prior to volatile exsolution may limit the ore-forming potential of the exsolving fluid and may contribute to the sporadic and relatively rare occurrence of magmatic-hydrothermal ore deposits in the crust at convergent margins. An alternative to sulfide saturation is loss of chalcophile elements into a hydrous phase during differentiation of the EMBB magmas [e.g., *Kamenetsky et al*., 2001; *Sun et al*., 2004, 2015]. Thus, the role

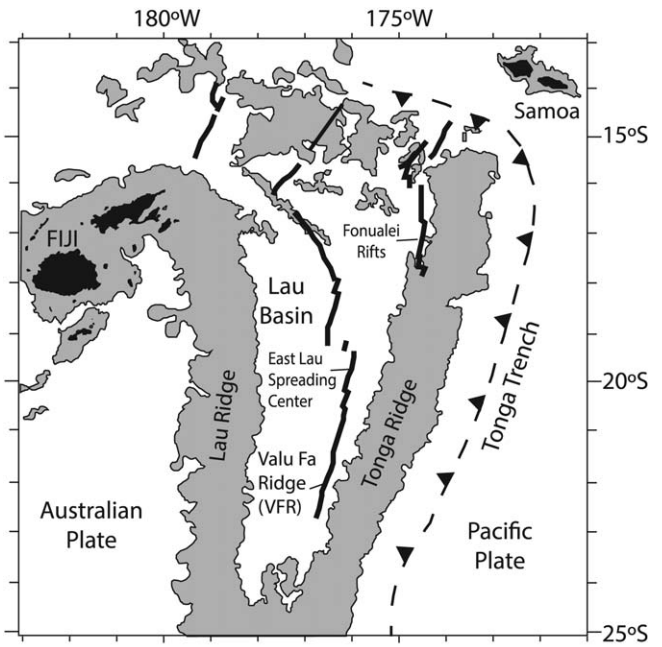

Figure 1. Map showing the major tectonic features of the Lau Basin. Areas of ocean floor shallower than 200 m are shaded gray (map modified from *Jenner et al.* [2012]). Data presented in this study are from the Valu Fa Ridge (VFR).

of sulfide saturation versus volatile exsolution on the partitioning of chalcophile elements during differentiation of hydrous convergent margin melts remains contentious.

Here we present major and trace element data for volcanic glass samples from the arc-proximal Valu Fa Ridge (VFR), Lau Back-arc Basin (sample locations shown in Figures 1 and 2 and given in supporting information Table 1). The axis of the ridge is oblique to the strike of the Tofua Arc volcanic front such that the southern propagating tip most closely approaches the front at ~40 km distance [*Collier and Sinha*, 1992; *Fretzdorff et al*., 2006]. The VFR can be separated into three major segments termed the Northern (NVFR), Central (CVFR), and Southern-Valu Fa Ridges (SVFR). The SVFR has been further divided into two major segments [*Massoth et al*., 2007]; the northern most segment we refer to here as the Hine Hina ridge (HHR) ridge and the southern most segment as the SVFR (Figure 2). The VFR erupts subalkaline (tholeiitic) basalt through to rhyolite compositions (see *Bach et al*. [1998], *Fretzdorff et al*. [2006], *Jenner et al*. [1987], *Kamenetsky et al*. [1997], and *Vallier et al*. [1991], which also include detailed petrological descriptions of samples erupting along the Valu Fa Ridge). In agreement with previous studies [e.g., *Kendrick et al*., 2014], we demonstrate that back-arc basin magmas erupting along the VFR are chemically similar to typical arc magmas. However, we suggest that their slightly lower volatile element contents prevent S degassing during differentiation, permitting the melts to achieve magnetite-triggered sulfide saturation. We suggest that the timing of volatile saturation relative to magnetite saturation in evolving convergent margin magmas may contribute to the sporadic occurrence of magmatic-hydrothermal ore deposits through the crust at convergent margins.

2. Results

The range in SiO_2, FeO_{TOT}, TiO_2, and V/Sc versus MgO of volcanic glass samples collected from the VFR are presented in Figure 3 (analytical techniques described in supporting information and data are presented in supporting information Tables 2–4, including previous major element analyses [*Goddard*, 2007; *Mikkelson*, 2005] of glass samples collected during the same voyage to the VFR). Glass samples from the VFR have a range in major element compositions from basalt to rhyolitic that is comparable to those from the EMBB and the Tonga-Kermadec arc (Figure 3). FeO_{TOT}, TiO_2, and V/Sc show an initial increase with decreasing MgO until ~4 wt % MgO, followed by a decrease with decreasing MgO.

Primitive (highest MgO, lowest SiO_2) samples from the VFR have comparable contents of Cu, Se, and Ag to primitive samples erupting in the EMBB, along the Tonga-Kermadec arc and the global MORB array (Figure 4). Samples from the SVFR show an increase in Cu, Se, and Ag with decreasing MgO, followed by an inflection in the trend at ~3 wt % MgO (Figure 4). This inflection, which is more clearly defined on the plot of SiO_2 versus Cu, Se, and Ag (Figure 4), is comparable to the liquid line of descent defined by the EMBB magmas. Samples from the HHR show a comparable trend in Cu, Se, and Ag versus MgO and SiO_2 to samples from the SVFR. In contrast, glasses from the CVFR (a single sample from dredge location Td 48 (NVFR) is discussed together with samples from the CVFR for ease of reference) show a scattered but broad decrease in Cu with decreasing MgO and increasing SiO_2.

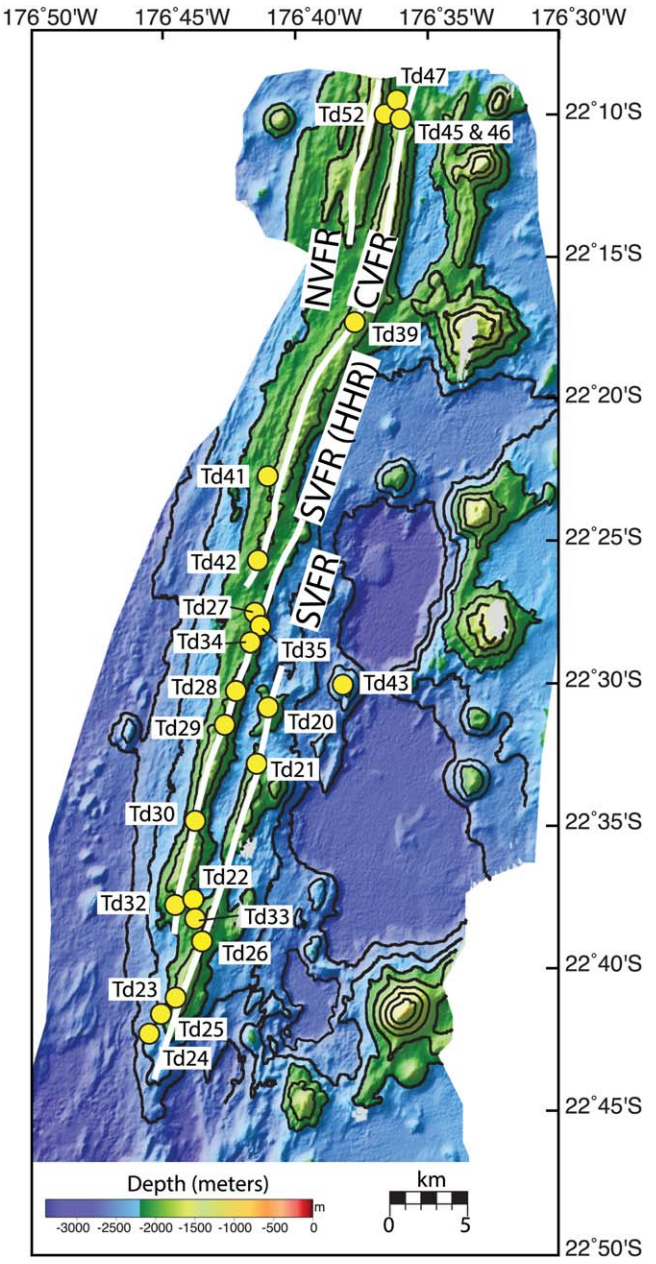

Figure 2. Multibeam sonar swath map of the Central Valu Fa Ridge (CVFR), Hine Hina Ridge (HHR), and Southern Valu Fa Ridge (SVFR) produced during the 2003 Tonga-Eastern Lau Vents Expedition (TELVE, SS02/03) of Australia's Marine National Facility RV *Southern Surveyor*: http://www.marine.csiro.au/nationalfacility/voyagedocs/2003/0203s.htm, showing locations of samples analyzed as part of this study.

Water contents range from 0.94 to 1.6 wt % and are significantly higher than MORB (Figure 5a). CO_2 contents are low, from 2 to 6 ppm, except for TD33-2 with 52 ppm CO_2 (Figure 5b). Sulfur contents range from 5 to 344 ppm and show a broad peak at ~4 wt % MgO (Figure 5c). Fluorine and chlorine behave as incompatible elements such as Ce, increasing with decreasing MgO (Figures 5d–5f). Trace element contents of the VFR samples normalized to primitive mantle (PM) show depletions in Nb and Ta and enrichments in Cs, Rb, and Ba relative to La (Figure 6). These trace element characteristics are comparable to those of magmas erupting along the neighboring Tonga-Kermadec arc (Figure 6) and in the EMBB (see PM-normalized diagram in *Jenner et al.* [2012]). Thus, although the samples analyzed and discussed here are from back-arc basins, their major and trace element characteristics are more similar to island arc magmas than MORB.

3. Discussion

3.1. Degassing During Eruption

The presence of vesicles in all samples collected from the VFR and EMBB and their low CO_2 contents indicate all magmas were volatile saturated on eruption. Loss of S during degassing of samples from the VFR is indicated by the higher S contents at a given MgO and FeO_{TOT} preserved in melt inclusions of similar composition in VFR near-axis seamounts [*Kamenetsky et al.*, 1997], compared to the volcanic glasses analyzed for this study (Figures 5c and 7a). A similar offset is also preserved between the majority of melt inclusions and glass samples from the EMBB [*Sun et al.*, 2004]. Despite evidence for S degassing, there is a correlation between S and FeO_{TOT} for samples from the VFR and the EMBB (Figure 7a), which is offset to lower S at a given FeO_{TOT} compared to the sulfide saturated MORB array. Depths of eruption of the VFR magmas (1640–2371 m) are comparable to those of MORB (730–5519 m, with an average (n = 329) eruption depth of 2992 m for MORB samples presented in Figure 7). These systematics imply melt composition rather than eruption pressure exerts the dominant control on the proportion of S exsolved from the melt during eruption-related degassing.

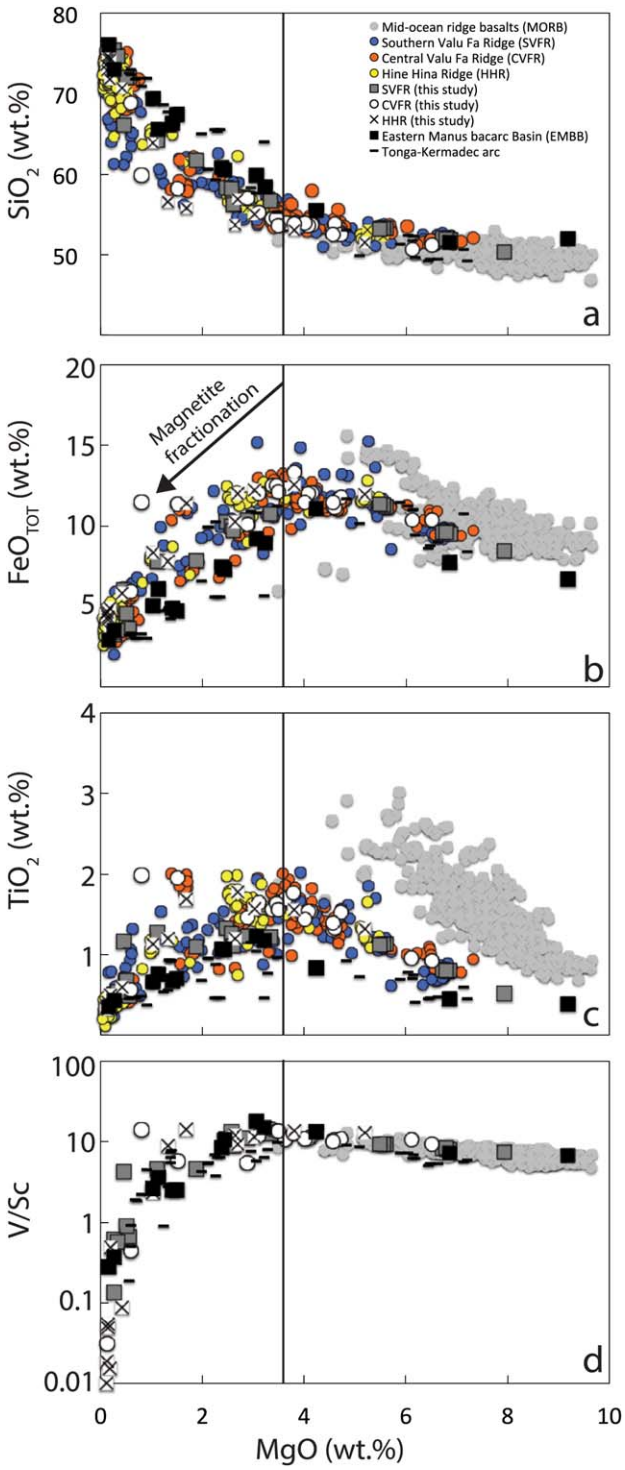

Figure 3. SiO_2, FeO_{TOT}, TiO_2, and V/Sc variations versus MgO for samples from the CVFR, HHR, and SVFR analyzed for this study and previous studies [*Goddard*, 2007; *Mikkelson*, 2005] compared to MORB [*Jenner and O'Neill*, 2012], samples from the EMBB [*Jenner et al.*, 2012] and the Tonga-Kermadec arc [*Dale et al.*, 2012; *Timm et al.*, 2012]. Samples from the VFR show a range in compositions comparable to those from the nearby Tonga-Kermadec arc. The inflection in the convergent margin differentiation trend between FeO_{TOT}, TiO_2, and V/Sc at ~3–4 wt % MgO is attributed to the fractionation of magnetite.

Like S, the solubility of CO_2 and H_2O in silicate melts is highly sensitive to pressure [e.g., *Dixon et al.*, 1995]. Most MORB have sufficiently low H_2O contents and are erupted at high enough hydrostatic pressures that they retain most of their magmatic budget of H_2O during eruption [*Michael*, 1995; *Moore*, 1970]. H_2O/Ce of MORB remain approximately constant with decreasing MgO, indicating similar compatibilities in the low-pressure fractionating phase assemblage and minimal H_2O degassing on eruption [e.g., *Cartigny et al.*, 2008; *Dixon et al.*, 2002; *Michael*, 1995]. In contrast to MORB, back-arc basin magmas from the VFR and EMBB show diverging H_2O and Ce behavior: H_2O remains approximately constant (Figure 5a), whereas Ce increases with decreasing MgO (Figure 5f), indicative of H_2O exsolution. The almost constant CO_2 and H_2O with decreasing MgO of both suites of back-arc basin magmas (Figure 5) can be attributed to the limited range in water pressures over which samples erupted (1640–2371 m). Hence, the primary magmatic H_2O of the VFR and EMBB is considered in excess of the range shown in Figure 5a (>1 wt %), demonstrating that both suites are typical volatile-laden convergent margin magmas. Excluding the sample with anomalously high CO_2 contents, the composition of the H_2O-CO_2 gas last in equilibrium with the VFR and EMBB magmas calculated using VolatileCalc [*Newman and Lowenstern*, 2002] ranges from 92 to 98 mol % H_2O and 2 to 8 mol % CO_2.

Seismic imaging [*Collier and Sinha*, 1992] places the depth to the top of the VFR magma chamber at 3.2 ± 0.2 km below the seafloor (dredge depths of 1730–2371 m). A similar depth has been inferred [*Moss and Scott*, 2001] for the magma chambers below the ridges at the EMBB (dredge depths of 1640–2000 m). At these pressures, the solubility of H_2O in the VFR magmas (and likely the

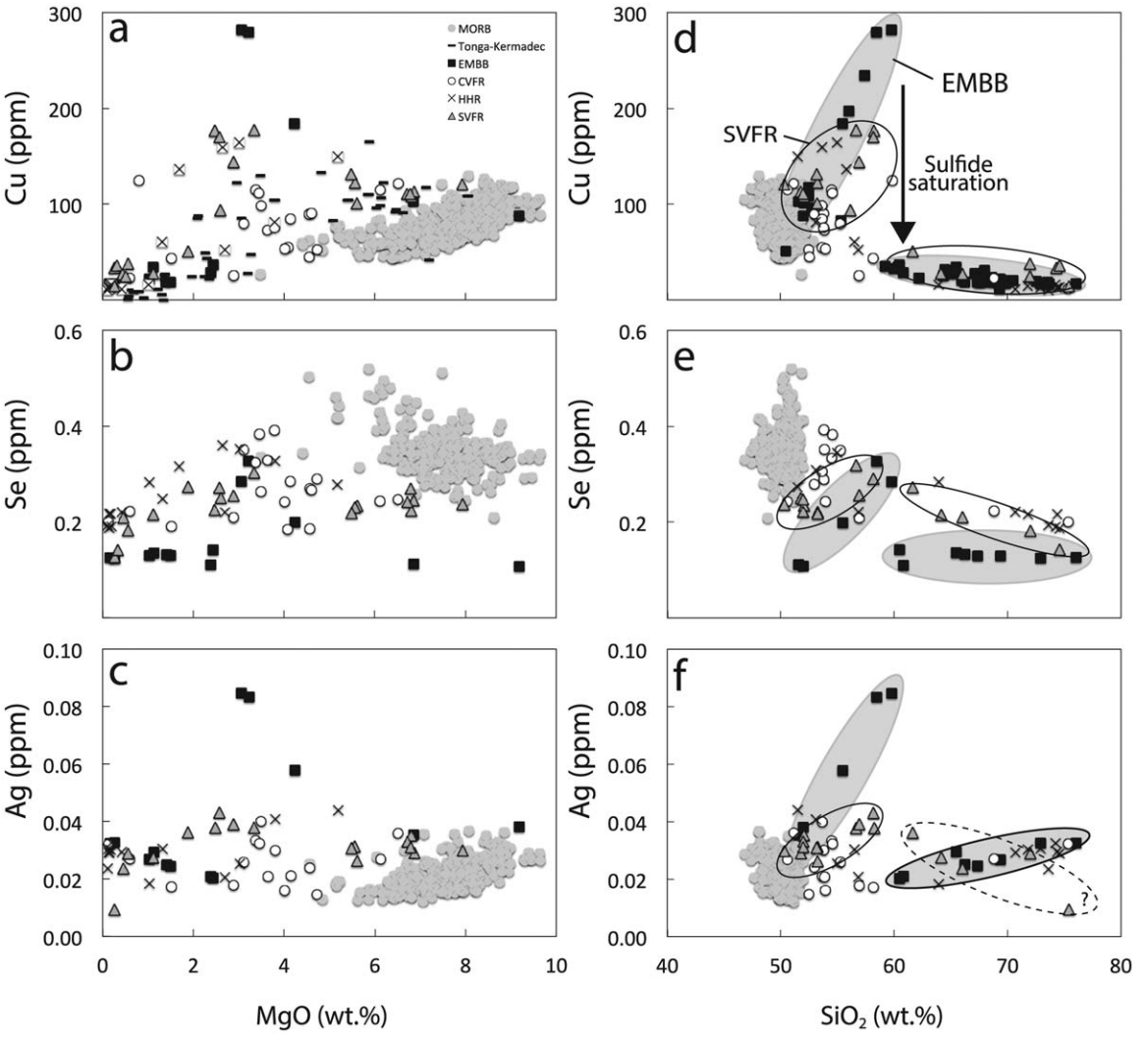

Figure 4. Variations in Cu, Se, and Ag versus MgO and SiO_2 for samples from the SVFR, HHR, CVFR, EMBB, and MORB and the Tonga-Kermadec arc. Data sources same as Figure 3, except Se in EMBB glasses given in supporting information Table 6. The inflection in the liquid line of descent for Cu, Se, and Ag at ~3 wt % MgO and ~60 wt % SiO_2 for samples from the SVFR and EMBB follows the onset of magnetite fractionation at 3–4 wt % MgO, indicating magnetite fractionation triggered sulfide saturation.

EMBB magmas) can be estimated using VolatileCalc to be 3.8 wt %. Hence, the VFR and EMBB magmas could have lost as much as 50% of their H_2O budget during eruption if the initial H_2O contents were as high as typical arc magmas worldwide [e.g., *Plank et al*., 2013].

In contrast to H_2O and CO_2, the contents of Cl and F increase markedly with decreasing MgO, similar to the highly incompatible lithophile element Ce (Figures 5d–5f), indicating that neither Cl nor F were partitioned extensively into the exsolving H_2O-CO_2 rich phase. Such trends are consistent with experimental studies which have shown Cl does not exsolve from the melt until extremely low pressures [*Lesne et al*., 2011] and with studies of volcanic gas and glass compositions, which suggest the onset of F degassing from the melt takes place at slightly lower pressures than Cl [*Edmonds et al*., 2009].

3.2. Chalcophile Element Budget of the Valu Fa Ridge Primitive Melts

The range in major element compositions, the high H_2O contents, and distinctive trace element patterns of the VFR back-arc basin magmas is strikingly similar to hydrous convergent margin magmas such as those erupting along the Tonga-Kermadec arc (Figures 3, 4, and 6). In particular, the high H_2O contents indicate that a proportion of the geochemical signatures of the VFR suite were inherited during hydrous fluxing of

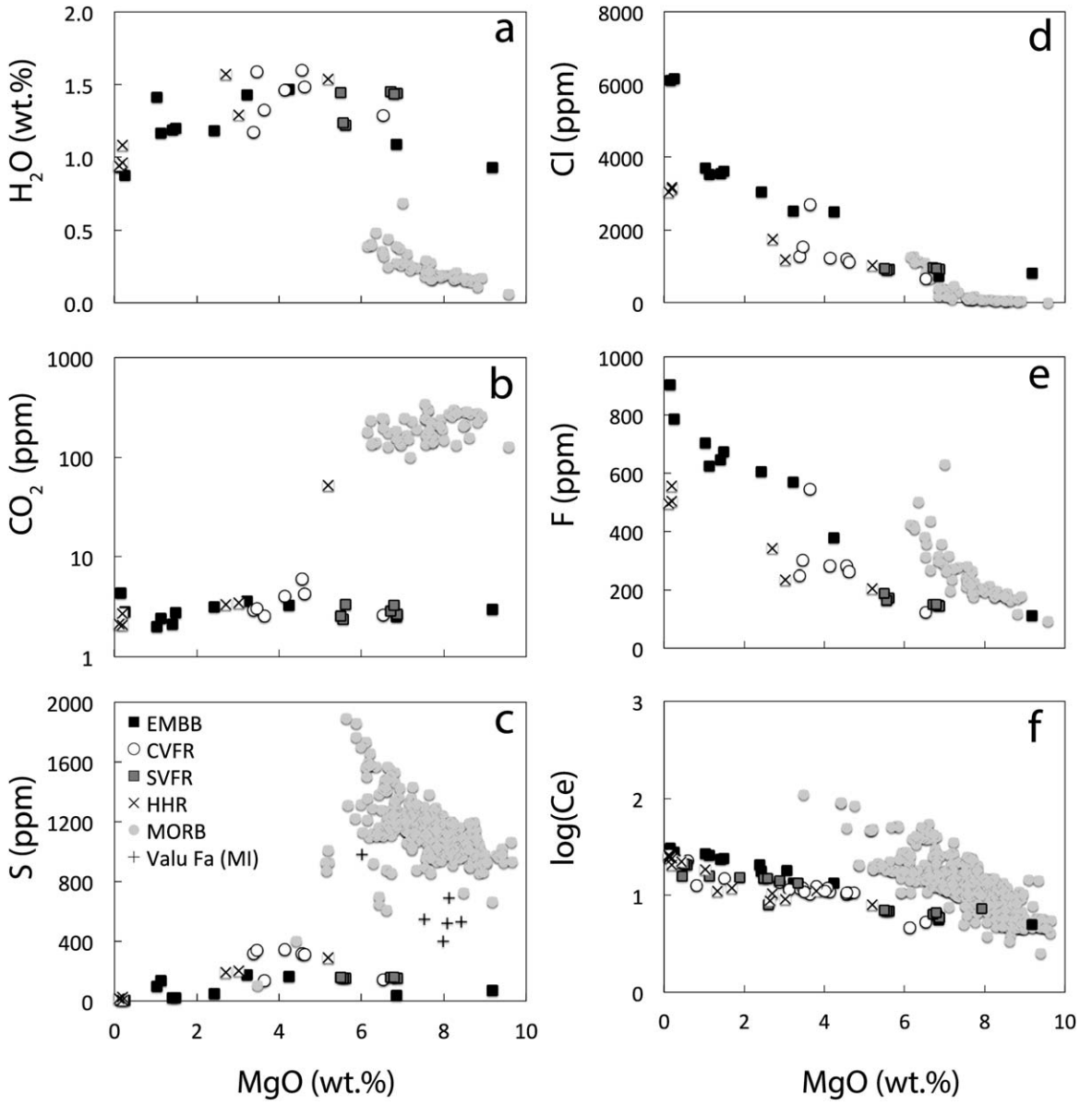

Figure 5. Variations in volatile and refractory lithophile (Ce) element abundances versus MgO for samples from the SVFR, CVFR, EMBB, and MORB. Data sources same as Figure 3 except MORB H_2O, CO_2, Cl, and F versus MgO contents from *le Roux et al*. [2006]. Samples from the VFR and EMBB have notably higher H_2O contents compared to MORB, indicating enrichment of the mantle source region during dehydration of the underlying subducting slab. The low CO_2 and S contents of samples from the VFR and EMBB compared to MORB and melt inclusions of similar composition in VFR near-axis seamounts [*Kamenetsky et al*., 1997], in addition to the almost constant H_2O contents, are consistent with volatile loss during eruption. In contrast to H_2O, CO_2, and S, the contents of F, Cl, and Ce increase with decreasing MgO, indicating negligible partitioning of both Cl and F into the exsolving volatile-rich phase.

the mantle wedge during subduction. In contrast to H_2O, the most primitive volcanic rocks from the VFR and the Tonga-Kermadec arc have concentrations of Cu, Se, and Ag that are either comparable or lower than primitive MORB (Figure 4), supporting previous conclusions that parental melts generated at convergent margins are not typically enriched in Cu and Ag [e.g., *Hamlyn et al*., 1985; *Jenner et al*., 2010; *Lee et al*., 2012]. In addition, the similarity in initial Cu contents between the VFR back-arc basin and the Tonga-Kermadec island arc samples indicate the proportion of Cu added to the mantle wedge during both shallow and deep subduction is negligible. Hence, it is likely that the partitioning of Cu, Ag, and Se during petrogenesis of convergent margin magmas is predominantly controlled by phases in the mantle wedge and not the subducting slab.

There is considerable disagreement in the literature regarding the role of residual sulfide melt, monosulfide solid solution (MSS), and/or silicate phases on the partitioning of Cu during the petrogenesis of MORB and

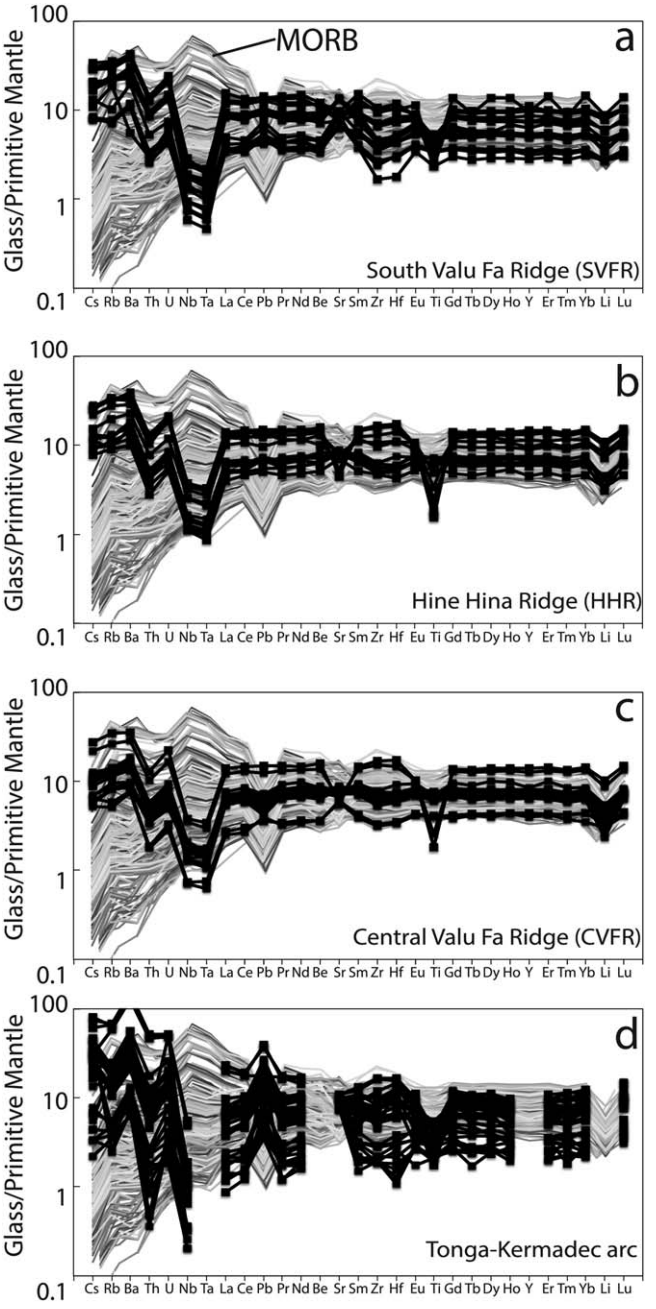

Figure 6. Primitive mantle normalized (values from *Palme and O'Neill* 2014) diagrams for samples from the CVFR, HHR, and SVFR and the Tonga-Kermadec arc compared to the MORB array. Data sources same as Figure 3. The comparable trace element patterns of samples from the VFR and EMBB compared to those from the Tonga-Kermadec arc as opposed to the MORB array (e.g., depletions in Nb relative to La) indicate the addition of a "slab-derived component" to the mantle wedge during the petrogenesis of the VFR and EMBB magmas.

arc basalts [e.g., *Jenner et al.*, 2010; *Lee et al.*, 2012; *Li*, 2014a; *Li and Audétat*, 2012; *Liu et al.*, 2014]. Sulfide-melt/silicate-melt partition coefficients (D) of Cu and Ag are almost identical at 951 ± 231 and 1005 ± 300, respectively, and are considerably higher than Se at 345 ± 37 [*Patten et al.*, 2013]. Unlike sulfide melt, which does not discriminate between Cu and Ag [*Jenner et al.*, 2010; *Kiseeva and Wood*, 2013; *Patten et al.*, 2013], available partition coefficients (D) show Cu is more compatible than Ag in MSS, clinopyroxene, garnet, and olivine [*Adam and Green*, 2006; *Li and Audétat*, 2012]. Hence, the comparable Cu/Ag of MORB compared to the VFR and EMBB suites (Figure 8) indicates that the budgets of Cu and Ag of samples erupted at each setting are dominated by residual sulfide melt in the mantle source region and not a crystalline sulfide or silicate phase. The lower Nb/Yb of convergent margin magmas compared to MORB is typically attributed to higher degrees of previous melt extraction from the mantle wedge compared to the MORB source mantle [*Pearce et al.*, 2005]. Hence, the higher Cu/Se and Ag/Se of primitive samples from the EMBB > VFR > MORB together with $D^{\text{sulfide melt/silicate melt}}$ imply Cu/Se and Ag/Se of mantle-derived melts can be used to track previous source depletion, with EMBB > VFR > MORB.

3.3. Discriminating Between the Roles of Sulfide, Magnetite, and Degassing on Chalcophile Element Partitioning

Recent studies have demonstrated the use of Cu-Ag-Se systematics for pinpointing the onset of sulfide saturation during low-pressure differentiation [*Jenner et al.*, 2010, 2012; *Patten et al.*, 2013]. In summary, MORB sulfides have higher Cu/Se and Ag/Se but comparable S/Se and Cu/Ag to MORB glasses (Figure 9). Hence, the decrease in Cu/Se and Ag/Se with decreasing MgO of the MORB array (Figure 9) indicates that sulfide saturation is reached by at least 9 wt % MgO, in agreement with the previous studies that consider MORB sulfide saturated on eruption [*Czamanske and Moore*, 1977; *Mathez*, 1976]. Samples from the EMBB with an fO_2 higher than MORB [*Sun et al.*, 2004] show an initial increase in the contents of Cu, Ag, and Se with decreasing MgO and increasing SiO_2 (Figure 4) and constant Cu/Se and Cu/Ag (Figure 8) until the appearance of magnetite on the liquidus at ~3–4 wt % MgO (Figure 3), implying that the evolving melts were initially sulfide

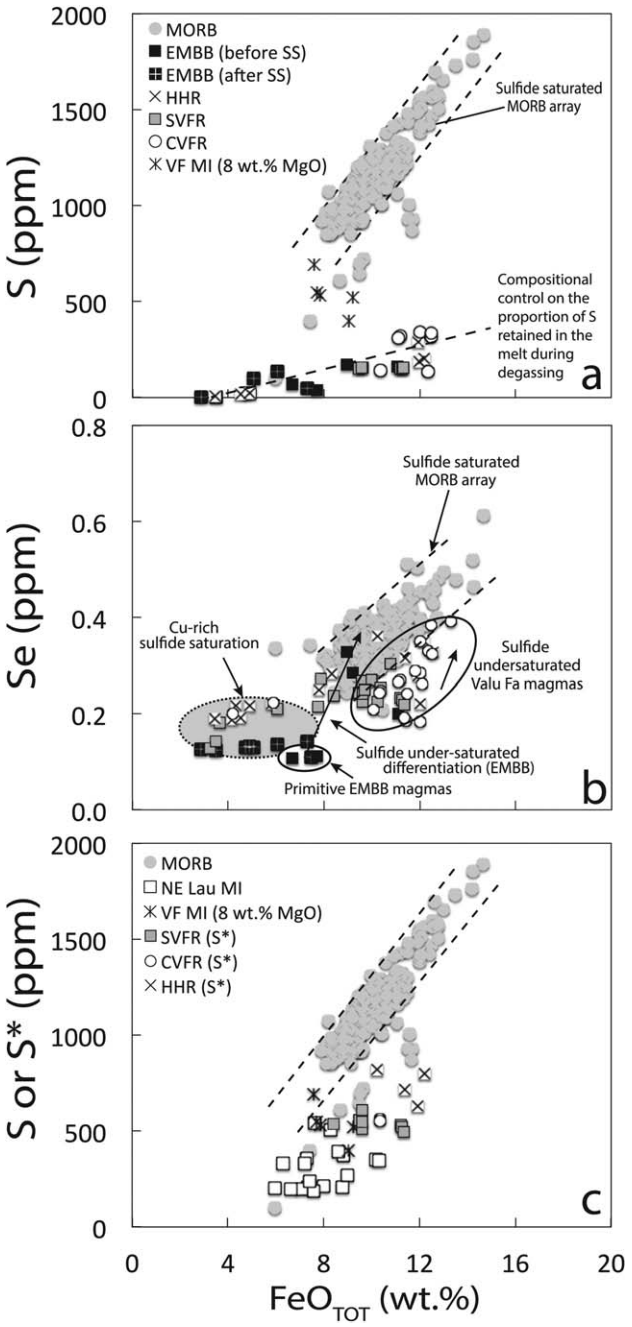

Figure 7. Chalcophile element systematic for samples from the CVFR, HHR, SVFR, EMBB, and MORB. Data sources same as Figure 4, except melt inclusion data from *Kamenetsky et al*. [1997]. (a) S versus FeO_{TOT}: glasses from the VFR have lower S contents at a given FeO_{TOT} compared to analyses of melt inclusions for samples from neighboring Valu Fa seamounts, indicating loss of S during eruption. The trend in S versus FeO_{TOT} for degassed samples from the VFR and EMBB indicate a compositional control on the proportion of S retained in the melt during degassing. (b) Se versus FeO_{TOT}: the majority of primitive samples from the VFR have lower Se at a given FeO_{TOT} compared to the MORB array, indicating Se is not added to the mantle wedge during subduction and (c) S or S* (S*=[Se] × S/Se_{MORB}) versus FeO_{TOT}: there is an increase in S* (glass) and S contents (melt inclusions) with increasing FeO_{TOT} for samples from the VFR that is offset to lower S at a given FeO_{TOT} compared to the MORB array, indicating the back-arc basin samples would have been sulfide undersaturated regardless of the likely higher fO_2 compared to MORB during differentiation. Melt inclusions hosted in minerals erupted in the rear arc of the NE Lau Basin (from *Park et al*. [2015]) also show low S contents at a given FeO_{TOT} compared to the MORB array, indicating Tonga arc samples are relatively S poor.

undersaturated [*Jenner et al*., 2010]. The sudden drop in Cu, Ag, Se, and Au, Cu/Se, and Ag/Se following the appearance of magnetite on the liquidus has been attributed to reduction-induced (magnetite crisis) sulfide saturation [*Jenner et al*., 2010]. Subsequently, *Park et al*. [2013] used the increase in Pd contents and constant Pd/Cu prior to magnetite fractionation and sudden decrease in Pd contents and Pd/Cu following magnetite fractionation as further evidence for the magnetite crisis during differentiation of the EMBB suite and rear arc samples erupting in the NE Lau Basin.

Differences in major element composition of samples immediately before (3.07 wt % MgO) and after (2.45 wt % MgO) the magnetite crisis were used to estimate only 2.6% magnetite removal from the EMBB melt during the interval wherein the 245 ppm drop in Cu contents takes place [*Jenner et al*., 2010]. Using the Rayleigh fractionation equation, this percentage removal of magnetite would require a $D_V^{magnetite/melt}$ of 22 to achieve the decrease in the content of V (Figure 10a), consistent with experimental partitioning studies for V [*Righter et al*., 2006; *Toplis and Corgne*, 2002]. Because of the low $D_{Cu}^{magnetite/melt}$ of 0.82–2.3 and $D_{Ag}^{magnetite/melt}$ of 2×10^{-4} [*Simon et al*., 2008], magnetite fractionation alone cannot account for the magnitude of the drop in Cu and Ag contents of 245 and 0.064 ppm, respectively (Figure 10a). Even at 10% magnetite fractionation, the modeled depletion in Cu is minor and such high percentages of magnetite fractionation would result in over-depletion of the melt in V (Figure 10a). Additionally, removal of magnetite alone cannot account for the concomitant drop in Se

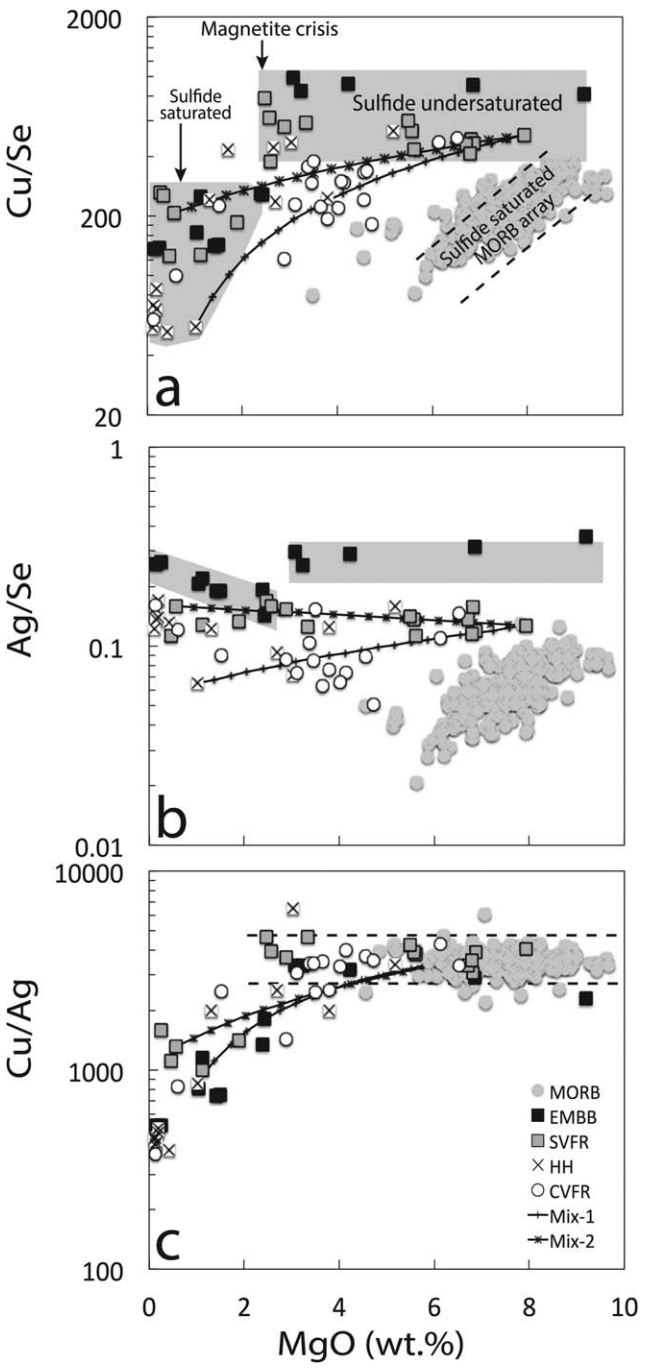

Figure 8. Variations in Cu/Se, Ag/Se, and Cu/Ag with changes in MgO for samples from the SVFR, HHR, CVFR, EMBB, and MORB. MORB shows a continual decrease in Cu/Se and Ag/Se but constant Cu/Ag with decreasing MgO, consistent with continual fractionation of sulfide melt. In contrast to MORB, between ~9 and ~3 wt % MgO, samples from the SVFR and the EMBB show constant Cu/Se and Ag/Se, indicating the evolving melts were sulfide undersaturated. At ~3 wt % MgO, there is a systematic decrease in Cu/Se and Cu/Ag for samples from the VFR and EMBB that follows magnetite fractionation at between 3 and 4 wt % MgO, indicating magnetite fractionation triggered saturation in a crystalline sulfide phase. Bulk magma mixing lines calculated using the most primitive (Td43-1) and most evolved (Td28-2 for mixing line 1 and Td21 for mixing line 2) samples from the SVFR (calculated in 5% mixing intervals). The compositions of samples from the CVFR plot on the mixing lines, indicating mixing between highly evolved (sulfide saturated) and primitive (sulfide undersaturated) magmas.

contents and implies saturation in a sulfide phase.

Unlike MORB, the EMBB shows a decrease in Cu/Ag following sulfide saturation (Figure 8c). Because sulfide-melt/silicate-melt partition coefficients of Cu and Ag are almost identical [*Patten et al.*, 2013], whereas crystalline sulfide preferentially partitions Cu relative to Ag [*Li and Audétat*, 2012], the decrease in Cu/Ag following magnetite fractionation has been attributed to saturation in a crystalline sulfide phase as opposed to sulfide melt [*Jenner et al.*, 2010, 2012; *Li*, 2014b; *Li and Audétat*, 2012; *Patten et al.*, 2013; *Wohlgemuth-Ueberwasser et al.*, 2012]. Fractionation of Cu from Ag can be achieved by magnetite fractionation, because $D_{Cu/Ag}^{magnetite/melt}$ is 4100 and 11,500 using the $D_{Cu}^{magnetite/melt}$ of 0.82 and 2.3, respectively [*Simon et al.*, 2008]. However, even at 10% magnetite removal, fractionation of Cu from Ag using these partition coefficients is minor and cannot reproduce the total decrease in Cu/Ag of the melt from 3333 (MD7b) to 1804 (MD53) required at the magnetite crisis (Figure 10b). For example, using the estimated percentage magnetite fractionation of 2.6% and assuming a $D_{Ag}^{magnetite/melt}$ of 2×10^{-4}, even at a hypothetical $D_{Cu}^{magnetite/melt}$ of 24 required to obtain the decrease in Cu/Ag, there is only a decrease in Cu in the melt of 126 ppm, and partitioning of 89 ppm Cu into the sulfide phase at saturation is still required (Figure 10b). Such a high $D_{Cu}^{magnetite/melt}$ is inconsistent with findings of experimental studies [*Simon et al.*, 2008] and analyses of Cu contents in magnetite (~3 ppm Cu) hosted in magmas erupting in the EMBB [*Sun et al.*, 2004]. Hence, the change in Cu/Ag at the magnetite crisis indicates that Cu was considerably more compatible in the sulfide phase than Ag and consequently this phase is unlikely to be sulfide melt.

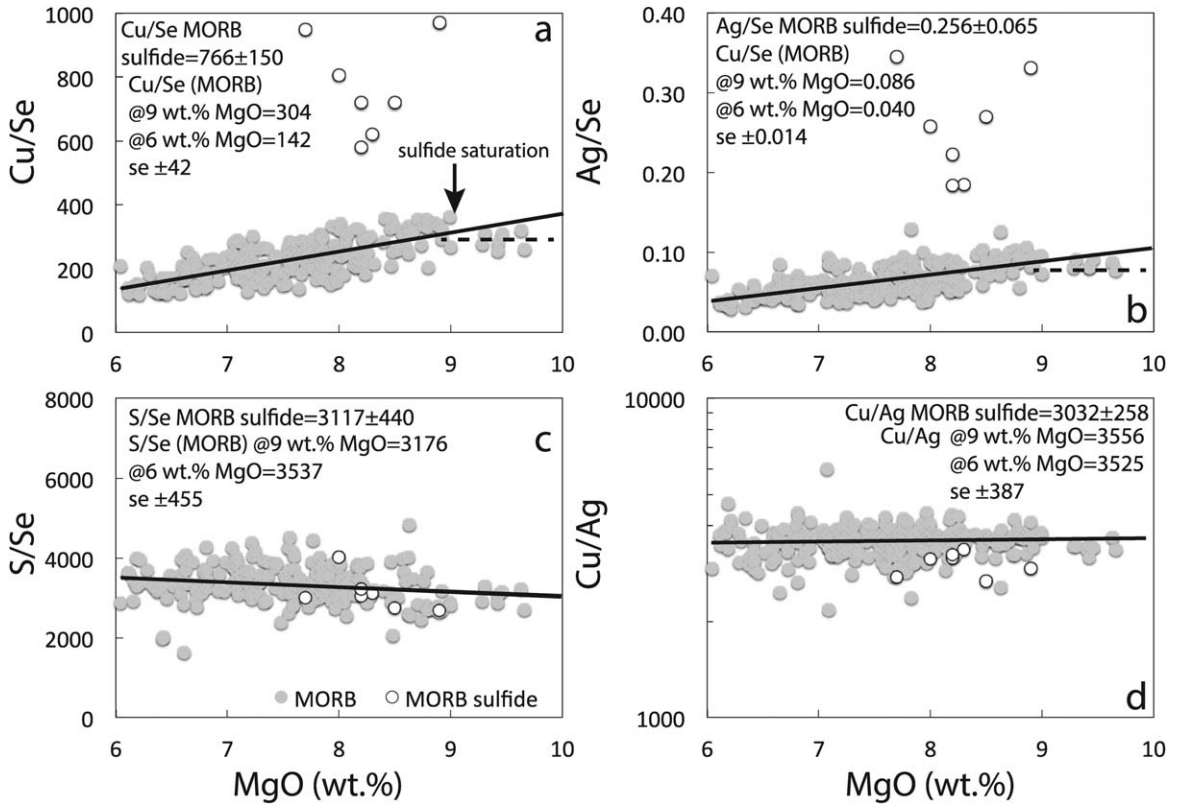

Figure 9. Variations in Cu/Se, Ag/Se, S/Se, and Cu/Ag with changes in MgO contents for MORB [*Jenner and O'Neill*, 2012] versus MORB sulfides [*Patten et al*., 2013] plotted using the MgO contents of the host glasses for sulfide analyses. The S/Se and Cu/Ag of sulfide melt and MORB glasses are within error, demonstrating that sulfide melt does not fractionate S from Se or Cu from Ag. The continual decrease in Cu/Se and Ag/Se indicates that MORB are sulfide saturated by at least 9 wt % MgO. Ratios are calculated from the intercepts of the slopes (e.g., Cu/Se versus MgO) at 9 wt % and at 6 wt % MgO to demonstrate the effects of sulfide fractionation on Cu/Se, Ag/Se, S/Se, and Cu/Ag during differentiation of MORB.

In contrast to Cu, Se, Ag, Pd, and Au, the contents of Ru, Rh, Ir, and Pt in the evolving EMBB magma systematically decrease with decreasing MgO both before and after magnetite fractionation [*Park et al*., 2013]. This decrease has been attributed to partitioning of the PGE into a Pt-rich alloy phase and Cr-spinel prior to magnetite fractionation, followed by partitioning into a sulfide phase at the magnetite crisis [*Park et al*., 2013]. *Park et al*. [2013] argued that the sulfide phase on the liquidus of the evolving EMBB magmas was not only enriched in Cu, but also the platinum group elements (PGE). *Park et al*. [2013] suggested a crystalline sulfide phase was unlikely to take all of the PGE into its structure and concluded that the sulfide phase on the liquidus must be melt. Indeed, a single elliptical shaped sulfide bleb hosted in magmas erupting in the NE Lau, which also show the magnetite crisis differentiation trend [*Park et al*., 2015], lends support for this conclusion. Alternatively, *Sun et al*. [2015] used the same reasoning to argue for direct partitioning of chalcophile elements into magmatic fluids instead of a sulfide phase. With the exception of Pd, following the EMBB magnetite crisis, there are no sudden drops in the contents of Ru, Rh, Ir, and Pt [*Park et al*., 2013, Figure 3]; the contents of Ru and Ir in the melt actually increase. It is only with further decreases in MgO content of the melt (i.e., postmagnetite crisis) that a decrease in the contents of the majority of the PGE is seen, suggesting a PGE-rich alloy fractionated from the EMBB both before and after, but potentially not during the magnetite crisis. We consider the preferential partitioning of Ag, Pd, and Au, which like Cu, occur as univalent ions in silicate melts as opposed to elements with higher valence states, such as Ni, Ru, Rh, Ir, and Pt [*Ertel et al*., 1999; *O'Neill et al*., 1995; *Tuff and O'Neill*, 2010; *Zajacz et al*., 2013] and notably, the decrease in Cu/Ag (not observed during differentiation of MORB) is consistent with the removal of a crystalline sulfide following magnetite-driven reduction of the melt. However, the sulfide bleb hosted in magmas erupting in the NE Lau Basin may suggest that both crystalline sulfide and sulfide melt were liquidus phases following magnetite fractionation. Because the decrease in Cu/Ag is consistent with experimental studies and analyses of natural sulfides, which demonstrate only crystalline sulfide fractionates Cu from Ag melt [*Kiseeva and Wood*, 2013; *Li*, 2014b; *Li and Audétat*, 2012; *Patten et al*., 2013], in the remainder of the text we use the term

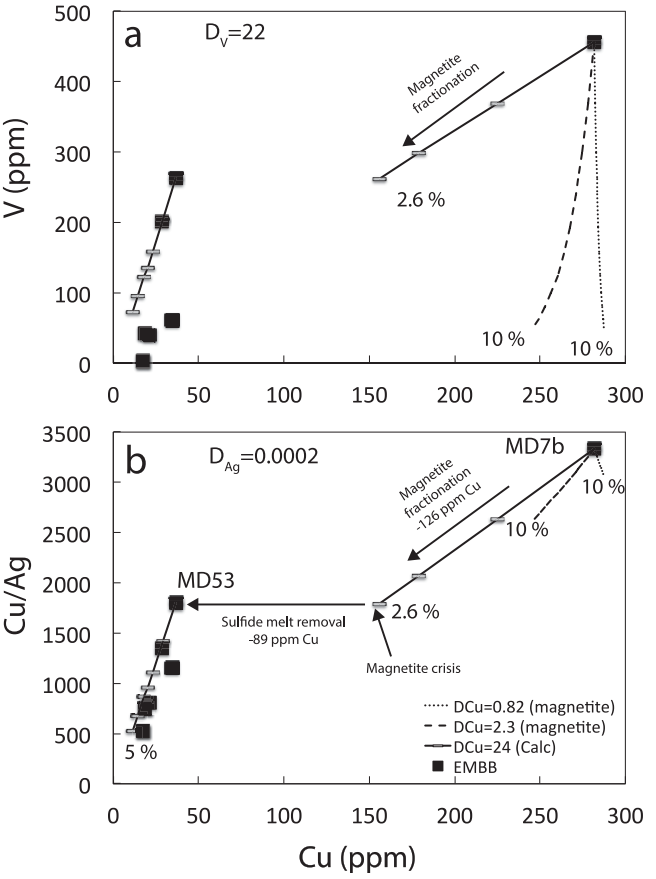

Figure 10. Variations in (a) V and (b) Cu/Ag versus Cu contents for samples from the EMBB compared to results of Rayleigh fractionation modeling. See text for discussion.

"crystalline sulfide" to emphasize the role of a high Cu/Ag sulfide phase that is compositionally distinct from the sulfide phase on the liquidus of MORB magmas. However, we note further petrological and geochemical studies of natural samples are required to confidently identify the type of sulfide on the liquidus that is causing the fractionation of Cu from Ag during differentiation of hydrous melts.

Other studies have attributed the decrease in Cu contents associated with magnetite fractionation in samples from the EMBB to the reduction of SO_4^{2-} to S^{2-} and the formation of Au-Cu-HS^- complexes which partition into high-temperature magmatic fluids and/or other mechanisms of degassing during differentiation and eruption [e.g., *Kamenetsky et al*., 2001; *Sun et al*., 2004, 2015; *Timm et al*., 2012]. The solubility of Cu in magmatic fluids has been shown to be several orders of magnitude higher than the PGE [*Wood*, 1987]. Consequently, if Cu was partitioned into magmatic fluids as opposed to a sulfide phase at the magnetite crisis, the Pd/Cu of the EMBB silicate melt would be expected to increase not decrease [*Park et al*., 2013]. *Sun et al*. [2015] argue that the proportion of S in the EMBB melt was too low to achieve sulfide saturation during differentiation. However, they did not consider (1) the effect of Cu on lowering the solubility of S in a melt, as discussed in detail in *Jenner et al*. [2010] or (2) the likely increase in S contents prior to the magnetite crisis (like Cu, Se, Ag, and Pd) from those preserved in the primitive melt inclusions.

The solubility of economically important elements such as Cu and Au in high temperature-pressure magmatic volatiles is strongly dependent on the availability of Cl [e.g., *Candela and Holland*, 1984; *Frank et al*., 2002; *Zajacz et al*., 2012]. Hence, the lack of Cl in the volatile phase may explain the apparent lack of mobility of Cu during degassing. However, analysis of Cl-rich gases and aerosols during eruption of the Tolbachik volcano, Kamchatka [*Zelenski et al*., 2014] show that Cu and Ag gas-magma partition coefficients are extremely low, implying Cu and Ag are not typically lost from the melt during eruption-triggered degassing. Because Cu-Se-Ag systematics of the EMBB suite are consistent with the removal of a sulfide phase during differentiation [*Jenner et al*., 2010; *Li*, 2014a; *Li and Audétat*, 2012; *Park et al*., 2013], we consider it unlikely that degassing of S and other volatiles took place during differentiation in the crust (i.e., volatiles were lost during degasing on eruption), otherwise the evolving melt would likely be too S-Cu-depleted to achieve sulfide saturation. Hence, it is likely that the H_2O contents of the EMBB magma during differentiation were slightly lower than the estimated ~3.8 wt % capacity of the melt, preventing volatile degassing during differentiation and permitting not only magnetite-triggered sulfide saturation, but also preservation of the distinct trend.

3.4. Sulfide Saturation During Differentiation of the SVFR and HHR Magmas

During differentiation of the SVFR magmas from ~8 to ~3 wt % MgO and ~50–60 wt % SiO_2, there is an increase in the contents of Cu, Se, and Ag (Figure 4), but Cu/Se, Ag/Se, and Cu/Ag remain approximately

constant (Figure 8), implying that the melts were initially sulfide undersaturated. With further decreases below ~3 wt % MgO and over ~60 wt % SiO_2, the SVFR magmas show a drop in the concentrations of Cu, Se, and Ag and a decrease in Cu/Se and Cu/Ag, consistent with the expected effects of crystalline sulfide saturation. The change in behavior of Cu, Se, and Ag follows an inflection in the liquid line of descent for FeO_{TOT}, TiO_2, and V/Sc at ~3–4 wt % MgO (Figure 3), suggesting the change in chalcophile element partitioning is attributable to magnetite (reduction)-triggered sulfide saturation and implying the evolving SVFR magmas had an fO_2 similar to that of the EMBB magmas. Our interpretation that the inflection in the FeO_{TOT}, TiO_2, and V/Sc liquid line of descent is attributable to magnetite fractionation is consistent with the observed phase assemblage [*Kamenetsky et al*., 1997; *Vallier et al*., 1991] and the phase assemblage expected during differentiation of hydrous melts [*Arculus*, 2004; *Sisson and Grove*, 1993; *Zimmer et al*., 2010]. During differentiation of the EMBB, the magnitude of the drop in Cu/Se at the magnetite crisis is more pronounced than Ag/Se, suggesting $D^{sulfide/silicate\ melt}$ for Cu > Ag > Se. However, there is no observed drop in Ag/Se during differentiation of the SVFR magmas (Figure 8), suggesting $D^{sulfide/silicate\ melt}$ for Ag and Se were identical and that there were subtle differences in the composition of the crystalline sulfide phase on the liquidus of the VFR and EMBB magmas.

A comparable differentiation trend is observed for the majority of samples from the HHR (Figure 8), indicating the magnetite crisis also occurred during differentiation of the HHR magmas. However, two samples from the HHR (Td29-3 and Td30) have notably lower Cu/Se (on account of their low Cu contents) compared to other >3 wt % MgO samples from the SVFR. The Cu/Se of these two samples are more akin to the compositions of samples erupted along the CVFR, which are discussed in the following section. Samples from the VFR and HHR were collected over a distance of >30 km (Figure 2). Hence, it is unlikely that the magmas were sourced from the same batch of magma. Consequently, the coherent liquid lines of descent indicate minimal variation in the parental melt compositions and differentiation histories between different batches of magmas erupting along the rift (i.e., the magnetite-triggered sulfide saturation is a common feature of the cooling history of the melts in the region and is unlikely to be an isolated event).

Loss of S during degassing of convergent margin magmas complicates interpretations regarding the behavior of S during magmatic differentiation in the crust. Because Se is not lost from the melt during degassing [*Hamlyn et al*., 1985; *Jenner et al*., 2010, 2012; *Wykes et al*., 2010], the abundance of S in sulfide undersaturated samples can be reconstructed (S*) from observed Se contents together with an estimate of the S/Se of the parental melt. The most primitive sample (8 wt % MgO) erupting along the VFR contains 0.237 ppm Se. The average S content of primitive melt inclusions (data from *Kamenetsky et al*. [1997]) with 8 wt % MgO (n = 5) is 538 ± 103 ppm, giving an estimate of the S/Se in the sulfide undersaturated melt of 2271 ± 436, which is slightly lower than that of MORB of 3176 ± 455 (Figure 8). Consequently, the content of S in sulfide undersaturated samples from the SVFR and HHR (excluding samples Td29-3 and Td30) prior to eruption can be estimated (S*) as 496–611 and 632–819 ppm, respectively (Figure 7). The slightly lower S and S* at a given FeO_{TOT} of the majority of pre-magnetite inclusions and glasses from the SVFR and HHR, compared to the MORB array suggests that the evolving magma(s) may have been initially sulfide undersaturated even if their fO_2 was similar to MORB. Mineral-hosted melt inclusions in magmas erupting at rear arc volcanoes in the NE Lau also plot at lower S contents at a given FeO compared to the MORB array (Figure 7c). Previous studies have suggested hydrous slab-derived components could deliver enough sulfate to the mantle wedge to cause the higher fO_2 of convergent margin magmas compared to MORB [e.g., *Kelley and Cottrell*, 2012]. However, the low S* and S of the Valu Fa Ridge and NE Lau magmas indicate that negligible S was added to the mantle wedge during the dehydration of the subducting slab that likely resulted in the higher H_2O contents of the melts (i.e., sulfate loss from the slab did not oxidize the overlying mantle wedge during subduction-related magmatism in the Lau Basin).

Fe-S-Se-Cu-Ag systematics of the VFR and EMBB suites appear to be in agreement with conclusions presented in previous studies, which suggest the mantle wedge may not be more oxidized than MORB during partial melting [e.g., *Lee et al*., 2012; *Mallmann and O'Neill*, 2009]. If a more oxidized mantle source is not involved, the most we can state is the requirement of magnetite-triggered-reduction of the melt to induce sulfide saturation during differentiation requires oxidation either en route from source to sites of crustal differentiation, or during the interval between intrusion of the melt into the crust and saturation in magnetite, such as crustal assimilation and/or fractional crystallization [e.g., *Cottrell and Kelley*, 2011]. Although

degassing of S as S^{4+} during differentiation can cause the fO_2 of a system to increase, this method of oxidation can only be achieved if the majority of the S was present as S^{6+} [*Metrich et al*., 2009] and the melt already had a higher fO_2 than MORB. Consequently, in addition to the necessity of minimal S degassing for the melt to achieve magnetite-triggered sulfide saturation, S degassing during differentiation is also unlikely to be the cause of the high fO_2 of the EMBB and potentially the VFR magmas compared to MORB. Hence, the timing and process(es) resulting in the differences in fO_2 between MORB and convergent margin magmas remain enigmatic and beyond the scope of this contribution.

3.5. Petrogenesis of the CVFR Magmas

Samples from the CVFR show more scatter on plots of Cu, Se, and Ag versus MgO and SiO_2 compared to samples from the SVFR, HHR, and EMBB (Figure 4). In addition, at a given SiO_2, many samples from the CVFR are offset to higher Se and lower Cu and Ag prior to magnetite fractionation compared to samples from the SVFR. The most primitive CVFR glasses have indistinguishable Cu/Se, Ag/Se, and Cu/Ag to primitive SVFR and HHR glasses indicating the compositions of the parental melts were comparable. However, glasses erupting along the CVFR show a broad decrease in Cu/Se (Figure 8a) with decreasing MgO, indicating the evolving melt(s) were sulfide-saturated prior to the onset of magnetite fractionation. This is in contrast to the SVFR and HHR magmas, where the decrease in Cu/Se follows the appearance of magnetite on the liquidus. However, the decrease in Cu/Ag of the CVFR magmas broadly coincides with the onset of magnetite fractionation (Figure 8c) and is similar to the decrease in Cu/Ag observed in sulfide-saturated samples erupting at the SVFR, HHR, and EMBB.

The apparent pre-magnetite crisis sulfide saturation during differentiation of the CVFR compared to the SVFR magmas may be the result of the former having an fO_2 during differentiation comparable to MORB (i.e., lower than the parental melts of the SVFR, HHR, and EMBB magmas) and/or higher initial S. However, the coincident inflection in V/Sc of melts erupting at the CVRF, SVFR, HHR, and EMBB indicates that the proportion of $Fe^{3+}/\Sigma Fe$ of the parental melts was comparable and dictated the timing of magnetite fractionation. Similarly, S* at a given FeO_{TOT} of the two most primitive (>6 wt % MgO) samples from the CVFR are comparable to those of the SVFR (Figure 7c) indicating the parental melts of both suites had similar S contents.

A compositional gap in anorthite contents of feldspars hosted by lavas erupting at the VFR has been attributed to mixing between evolved and more mafic melts during recharging of magma chambers [*Vallier et al*., 1991]. Mixing of a highly evolved sulfide-saturated melt (Td28-2 and Td21) with primitive sulfide undersaturated melts (i.e., Td43-1) would result in a continuous range in Cu/Se with decreasing MgO, as opposed to the sudden drop in Cu/Se following sulfide saturation in samples from the SVFR, HHR, and EMBB (see mixing lines in Figure 8). The range in Cu/Se, Ag/Se, and Cu/Ag and highly variable Se, Cu, Ag, and major element contents (Figures 4 and 8) of the CVFR suite are consistent with the range expected by mixing of S-saturated evolved melts with S undersaturated primitive melts. Because there are no obvious differences between the likely fO_2 or S* of samples from the CVFR compared to the SVFR and HHR, magma mixing provides a simple solution to the contradictory chalcophile element systematics of the former. If the magma chambers below the SVFR and HHR were also recharging during differentiation, both the evolved and primitive melts must have been sulfide undersaturated (e.g., the evolved melts had MgO contents >4 wt % MgO) to permit preservation of the magnetite-crisis trend. Indeed, the overenrichment effects of recharge on incompatible element abundances [e.g., *Lee et al*., 2013; *O'Neill and Jenner*, 2012] may explain the evolution to higher Cu of the EMBB compared to the SVFR magmas prior to magnetite saturation (Figure 4).

Differences in differentiation trends between magmas sourced beneath the tip and beneath the more mature part of the Galapagos spreading center have been attributed to evolution of the system at the tip from small, isolated magma chambers through to increasingly large and interconnected chambers, to steady state buffered systems in the mature parts of the spreading center [*Christie and Sinton*, 1981]. Evidence for magma mixing in the CVFR and not the SVFR and HHR may indicate that magma supply to the more topographically prominent and mature part of the Ridge was more frequent than at the propagating tip (SVFR). Magmas erupting at propagating tips of spreading ridges (such as the SVFR and EMBB), where magma supply might be lower/more sporadic, may permit melts to evolve to higher silica contents compared to more mature parts of the rift, permitting the preservation of the magnetite-crisis trend.

4. Implications and Conclusions

We attribute the systematic change in chalcophile element behavior at ~3 wt % MgO to magnetite-triggered sulfide saturation during differentiation of the SVFR and HHR magmas. Because many convergent margin magmas are geochemically similar to the SVFR, HHR, and EMBB magmas (i.e., evolve past magnetite fractionation and have comparable volatile (H_2O), chalcophile and other trace element concentrations), the magnetite crisis may be a common aspect to the differentiation history of many convergent margin magmas. The identification of this process in other convergent margin settings worldwide may have gone unnoticed because of the dearth of Cu, Se, and Ag analyses of volcanic glass samples in the literature. Additionally, the likelihood of magma recharge events in mature convergent margin systems [e.g., *Lee et al*., 2013], resulting in the mixing between sulfide saturated and sulfide undersaturated melts, likely obscures identification of the magnetite-crisis trend.

Previous studies have argued that sulfide removal prior to vapor saturation is likely to decrease the probability of forming economically viable deposits [e.g., *Candela and Holland*, 1986]. Because the magnetite crisis will result in the storage of a large proportion of the chalcophile element budget of a system in magmatic sulfides, this process may provide a potential clue to why many intrusions sourced by convergent margin magmas are barren. Hence, melts that do not "suffer" a magnetite crisis may be more likely to be associated with Cu-rich mineralization. For example, in the likely case that (a) an evolving melt had slightly higher initial volatile contents than the EMBB and VFR magmas, or differentiated at lower pressures, permitting volatile saturation during crustal differentiation (as seems the case for many convergent margin magmas) [see *Plank et al*., 2013, for example] as opposed to only during eruption (as appears to be the case for the VFR and EMBB suites), and as a consequence, (b) the magma degassed the majority of its sulfur prior to the onset of magnetite fractionation: there might not be enough S and/or Cu in the melt to reach sulfide saturation following magnetite fractionation. This scenario would likely be favorable to continual exsolution of a metal-rich, potentially ore-forming fluid. If most melts evolving in the continental crust are indeed volatile saturated, the magnetite crisis event may instead be rare and restricted to less volatile-rich magmas, such as those erupting in the back-arc setting. However, because the solubility of H_2O and CO_2 in a silicate melt increases with depth [*Dixon et al*., 1995], whereas the solubility of S decreases with depth [*Mavrogenes and O'Neill*, 1999], the magnetite crisis might also occur during differentiation of volatile-rich convergent margin magmas at high pressures in the continental crust. For example, magmas that source magmatic-hydrothermal ore deposits, such as porphyry ore deposits, are typically thought to stall in the crust at 6–10 km depth [*Cooke et al*., 2014; *Wilkinson*, 2013], potentially indicating melts evolving at pressures >10 km reach the magnetite crisis prior to H_2O-CO_2 saturation, which in turn limits the proportion of chalcophile element that partition into the exsolving phase.

Seafloor hydrothermal sulfide deposits have been documented at both the EMBB [*Binns and Scott*, 1993] and at the VFR [*Fretzdorff et al*., 2006], indicating that magmatism in both settings is in some way linked to the occurrence of sulfide deposits in the region. The systematic variations in F, Cl, Cu/Se, Ag/Se, and Cu/Ag with variations in MgO of the VFR and EMBB suites suggest that Cl, F, Cu, Ag, and Se were unlikely to be partitioning into the exsolving volatile phase during eruption-related degassing. Hence, it is unlikely that the overlying seafloor mineralization in both settings and neighboring areas can be directly attributed to exsolution of Cu-rich magmatic fluids, as suggested by previous studies [*Kamenetsky et al*., 2001; *Sun et al*., 2004; *Timm et al*., 2012]. Late-stage magnetite-triggered sulfide saturation during differentiation of both the SVF and EMBB magmas may concentrate sulfides in the upper, more evolved portions of magma chambers, making them highly susceptible to leaching by circulating seawater. In addition, the Cu-rich nature of the sulfide phases may enhance the probability that circulating seawater scavenges Cu, Ag, and Au from the host rock, and it is these leaching processes and later precipitation that is the dominant cause of mineralization on the sea floor at the VFR and EMBB.

Acknowledgments

Major and trace element data for samples from the VFR are presented in supporting information. We thank the officers, crew, and coscientific staff of the *RV Southern Surveyor* 02/2003 Tonga-Eastern Lau Vents Expedition for their effort in retrieving samples from the Valu Fa Ridge that were analyzed as part of this study. The postvoyage analytical costs for analyses undertaken at the RSES were supported by an Australian Research Council Discovery Grant to Richard Arculus and John Mavrogenes. Frances Jenner and Erik Hauri acknowledge funding from the Deep Carbon Observatory and the DTM for analyses undertaken at the DTM. We thank Jianhua Wang, Tim Mock, and Charlotte Allen for expert maintenance and assistance in the DTM SIMS lab and LA-ICPMS facility at the RSES, ANU, respectively. Ed Mathez, Sune Nielsen, and an anonymous reviewer are thanked for taking the time to review our manuscript and for their constructive criticism that improved the clarity of the text. Jannes Blichert-Toft is thanked for the editorial handing of our manuscript and constructive criticism throughout the submission process.

References

Adam, J., and T. Green (2006), Trace element partitioning between mica- and amphibole-bearing garnet lherzolite and hydrous basanitic melt: 1. Experimental results and the investigation of controls on partitioning behaviour, *Contrib. Mineral. Petrol.*, *152*(1), 1–17, doi: 10.1007/s00410-006-0085-4.

Arculus, R. J. (2004), Evolution of arc magmas and their volatiles, in *The State of the Planet: Frontiers and Challenges in Geophysics*, edited by R. S. J. Sparks and C. J. Hawkesworth, pp. 95–108, AGU, Washington, D. C.

Audétat, A., T. Pettke, C. A. Heinrich, and R. J. Bodnar (2008), Special paper: The composition of magmatic-hydrothermal fluids in barren and mineralized intrusions, *Econ. Geol.*, *103*(5), 877–908, doi:10.2113/gsecongeo.103.5.877.

Bach, W., E. Hegner, and J. Erzinger (1998), Chemical fluxes in the Tonga subduction zone: Evidence from the Southern Lau Basin, *Geophys. Res. Lett.*, *25*(9), 1467–1470, doi:10.1029/98GL00840.

Binns, R. A., and S. D. Scott (1993), Actively forming polymetallic sulfide deposits associated with felsic volcanic rocks in the eastern Manus back-arc basin, Papua New Guinea, *Econ. Geol.*, *88*(8), 2226–2236, doi:10.2113/gsecongeo.88.8.2226.

Blundy, J., J. Mavrogenes, B. Tattitch, S. Sparks, and A. Gilmer (2015), Generation of porphyry copper deposits by gas-brine reaction in volcanic arcs, *Nat. Geosci.*, *8*, 235–240, doi:10.1038/ngeo2351.

Bodnar, R. J., P. Lecumberri-Sanchez, D. Moncada, and M. Steele-MacInnis (2014), Fluid inclusions in hydrothermal ore deposits, in *Treatise on Geochemistry*, edited by H. D. Holland and K. K. Turekian, vol. 13, 2nd ed., chap. 5, pp. 119–142, Elsevier, Oxford, U. K.

Bosi, F., U. Hålenius, and H. Skogby (2009), Crystal chemistry of the magnetite-ulvöspinel series, *Am. Mineral.*, *94*(1), 181–189, doi:10.2138/am.2009.3002.

Candela, P. A., and H. D. Holland (1984), The partitioning of copper and molybdenum between silicate melts and aqueous fluids, *Geochim. Cosmochim. Acta*, *48*(2), 373–380, doi:10.1016/0016-7037(84)90257-6.

Candela, P. A., and H. D. Holland (1986), A mass transfer model for copper and molybdenum in magmatic hydrothermal systems: The origin of porphyry-type ore deposits, *Econ. Geol.*, *81*(1), 1–19, doi:10.2113/gsecongeo.81.1.1.

Carmichael, I. E. (1991), The redox states of basic and silicic magmas: A reflection of their source regions?, *Contrib. Mineral. Petrol.*, *106*(2), 129–141, doi:10.1007/bf00306429.

Carmichael, I. S. E. (1967), The iron-titanium oxides of salic volcanic rocks and their associated ferromagnesian silicates, *Contrib. Mineral. Petrol.*, *14*, 36–64.

Cartigny, P., F. Pineau, C. Aubaud, and M. Javoy (2008), Towards a consistent mantle carbon flux estimate: Insights from volatile systematics (H_2O/Ce, δD, CO_2/Nb) in the North Atlantic mantle (14°N and 34°N), *Earth Planet. Sci. Lett.*, *265*(3–4), 672–685, doi:10.1016/j.epsl.2007.11.011.

Christie, D. M., and J. M. Sinton (1981), Evolution of abyssal lavas along propagating segments of the Galapagos spreading center, *Earth Planet. Sci. Lett.*, *56*, 321–335, doi:10.1016/0012-821X(81)90137-0.

Cline, J. S., and R. J. Bodnar (1991), Can economic porphyry copper mineralization be generated by a typical calc-alkaline melt?, *J. Geophys. Res.*, *96*(B5), 8113–8126, doi:10.1029/91JB00053.

Collier, J. S., and M. C. Sinha (1992), Seismic mapping of a magma chamber beneath the Valu Fa Ridge, Lau Basin, *J. Geophys. Res.*, *97*(B10), 14,031–14,053, doi:10.1029/91JB02751.

Cooke, D. R., P. Hollings, J. J. Wilkinson, and R. M. Tosdal (2014), Geochemistry of porphyry deposits, in *Treatise on Geochemistry*, edited by H. D. Holland and K. K. Turekian, vol. 13, 2nd ed., chap. 14, pp. 357–381, Elsevier, Oxford, U. K.

Cottrell, E., and K. A. Kelley (2011), The oxidation state of Fe in MORB glasses and the oxygen fugacity of the upper mantle, *Earth Planet. Sci. Lett.*, *305*, 270–282, doi:10.1016/j.epsl.2011.03.014.

Czamanske, G. K., and J. G. Moore (1977), Composition and phase chemistry of sulfide globules in basalts from the Mid-Atlantic-Ridge rift valley near 37°N lat, *Geol. Soc. Am. Bull.*, *88*, 587–599, doi:10.1130/0016-7606(1977)88<587:CAPCOS>2.0.CO;2.

Dale, C. W., C. G. Macpherson, D. G. Pearson, S. J. Hammond, and R. J. Arculus (2012), Inter-element fractionation of highly siderophile elements in the Tonga Arc due to flux melting of a depleted source, *Geochim. Cosmochim. Acta*, *89*, 202–225, doi:10.1016/j.gca.2012.03.025.

Dixon, J. E., E. M. Stolper, and J. R. Holloway (1995), An experimental study of water and carbon dioxide solubilities in Mid-Ocean Ridge basaltic liquids. Part I: Calibration and solubility models, *J. Petrol.*, *36*, 1607–1631.

Dixon, J. E., L. Leist, C. Langmuir, and J.-G. Schilling (2002), Recycled dehydrated lithosphere observed in plume-influenced mid-ocean-ridge basalt, *Nature*, *420*(6914), 385–389, doi:10.1038/nature01215.

Edmonds, M., T. M. Gerlach, and R. A. Herd (2009), Halogen degassing during ascent and eruption of water-poor basaltic magma, *Chem. Geol.*, *263*(1–4), 122–130, doi:10.1016/j.chemgeo.2008.09.022.

Ertel, W., H. St. C. O'Neill, P. J. Sylvester, and D. B. Dingwell (1999), Solubilities of Pt and Rh in a haplobasaltic silicate melt at 1300°C, *Geochim. Cosmochim. Acta*, *63*(16), 2439–2449, doi:10.1016/S0016-7037(99)00136-2.

Frank, M. R., P. A. Candela, P. M. Piccoli, and M. D. Glascock (2002), Gold solubility, speciation, and partitioning as a function of HCl in the brine-silicate melt-metallic gold system at 800°C and 100 MPa, *Geochim. Cosmochim. Acta*, *66*(21), 3719–3732, doi:10.1016/S0016-7037(01)00900-0.

Fretzdorff, S., U. Schwarz-Schampera, H. L. Gibson, C. D. Garbe-Schönberg, F. Hauff, and P. Stoffers (2006), Hydrothermal activity and magma genesis along a propagating back-arc basin: Valu Fa Ridge (southern Lau Basin), *J. Geophys. Res.*, *111*, B08205, doi:10.1029/2005JB003967.

Goddard, C. (2007), *Geochemical and helium isotopic variability within the Lau Basin*, Ph.D. dissertation, 262 pp., Oreg. State Univ., Corvallis.

Hamlyn, P. R., R. R. Keays, W. E. Cameron, A. J. Crawford, and H. M. Waldron (1985), Precious metals in low-Ti lavas: Implications for metallogenesis and sulfur saturation in primary magmas, *Geochim. Cosmochim. Acta*, *49*(8), 1797–1811, doi:10.1016/0016-7037(85)90150-4.

Hedenquist, J. W., and J. B. Lowenstern (1994), The role of magmas in the formation of hydrothermal ore deposits, *Nature*, *370*, 519–527.

Hildreth, W. (1983), The compositionally zoned eruption of 1912 in the valley of ten thousand smokes, Katmai National Park, Alaska, *J. Volcanol. Geotherm. Res.*, *18*(1–4), 1–56, doi:10.1016/0377-0273(83)90003-3.

Jenner, F. E., and H. St. C. O'Neill (2012), Analysis of 60 elements in 616 ocean floor basaltic glasses, *Geochem. Geophys. Geosyst.*, *13*, Q02005, doi:10.1029/2011GC004009.

Jenner, F. E., H. St. C. O'Neill, R. J. Arculus and J. A. Mavrogenes (2010), The magnetite crisis in the evolution of arc-related magmas and the initial concentration of Au, Ag, and Cu, *J. Petrol.*, *51*(12), 2445–2464, doi:10.1093/petrology/egq063.

Jenner, F. E., R. J. Arculus, J. A. Mavrogenes, N. J. Dyriw, O. Nebel and E. H. Hauri (2012), Chalcophile element systematics in volcanic glasses from the Northwestern Lau Basin, *Geochem. Geophys. Geosyst.*, *13*, Q06014, doi:10.1029/2012GC004088.

Jenner, G. A., P. A. Cawood, M. Rautenschlein, and W. M. White (1987), Composition of back-arc basin volcanics, Valu Fa Ridge, Lau Basin: Evidence for a slab-derived component in their mantle source, *J. Volcanol. Geotherm. Res.*, *32*(1–3), 209–222, doi:10.1016/0377-0273(87)90045-X.

Jugo, P. J. (2009), Sulfur content at sulfide saturation in oxidized magmas, *Geology*, *37*(5), 415–418, doi:10.1130/G25527A.1.

Kamenetsky, V. S., A. J. Crawford, S. Eggins, and R. Mühe (1997), Phenocrysts and melt inclusion chemistry of near-axis seamounts, Valu Fa Ridge, Lau Basin: Insight into mantle wedge melting and the addition of subduction components, *Earth Planet. Sci. Lett.*, *151*, 205–223, doi:10.1016/S0012-821X(97)81849-3.

Kamenetsky, V. S., R. A. Binns, J. B. Gemmell, A. J. Crawford, T. P. Mernagh, R. Maas, and D. Steele (2001), Parental basaltic melts and fuids in eastern Manus backarc basin: Implications for hydrothermal mineralisation, *Earth Planet. Sci. Lett.*, *184*, 685–702, doi:10.1016/S0012-821X(00)00352-6.

Kelley, K. A., and E. Cottrell (2009), Water and the oxidation state of subduction zone magmas, *Science*, *325*(5940), 605–607, doi:10.1126/science.1174156.

Kelley, K. A., and E. Cottrell (2012), The influence of magmatic differentiation on the oxidation state of Fe in a basaltic arc magma, *Earth Planet. Sci. Lett.*, *329–330*, 109–121, doi:10.1016/j.epsl.2012.02.010.

Kendrick, M. A., R. J. Arculus, L. V. Danyushevsky, V. S. Kamenetsky, J. D. Woodhead, and M. Honda (2014), Subduction-related halogens (Cl, Br and I) and H_2O in magmatic glasses from Southwest Pacific Backarc Basins, *Earth Planet. Sci. Lett.*, *400*, 165–176, doi:10.1016/j.epsl.2014.05.021.

Kiseeva, E. S., and B. J. Wood (2013), A simple model for chalcophile element partitioning between sulphide and silicate liquids with geochemical applications, *Earth Planet. Sci. Lett.*, *383*, 68–81, doi:10.1016/j.epsl.2013.09.034.

le Roux, P. J., S. B. Shirey, E. H. Hauri, M. R. Perfit, and J. F. Bender (2006), The effects of variable sources, processes and contaminants on the composition of northern EPR MORB (8–10°N and 12–14°N): Evidence from volatiles (H_2O, CO_2, S) and halogens (F, Cl), *Earth Planet. Sci. Lett.*, *251*(3–4), 209–231, doi:10.1016/j.epsl.2006.09.012.

Lee, C.-T. A., P. Luffi, E. J. Chin, R. Bouchet, R. Dasgupta, D. M. Morton, V. Le Roux, Q.-Z. Yin, and D. Jin (2012), Copper systematics in arc magmas and implications for crust-mantle differentiation, *Science*, *336*(6077), 64–68, doi:10.1126/science.1217313.

Lee, C.-T. A., T. C. Lee, and C.-T. Wu (2013), Modeling the compositional evolution of recharging, evacuating, and fractionating (REFC) magma chambers: Implications for differentiation of arc magmas, *Geochim. Cosmochim. Acta*, *143*, 8–22, doi:10.1016/j.gca.2013.08.009.

Lesne, P., S. C. Kohn, J. Blundy, F. Witham, R. E. Botcharnikov, and H. Behrens (2011), Experimental simulation of closed-system degassing in the system basalt-H_2O-CO_2-S-Cl, *J. Petrol.*, *52*(9), 1737–1762, doi:10.1093/petrology/egr027.

Li, Y. (2014a), Chalcophile element partitioning between sulfide phases and hydrous mantle melt: Applications to mantle melting and the formation of ore deposits, *J. Asian Earth Sci.*, *94*, 77–93, doi:10.1016/j.jseaes.2014.08.009.

Li, Y. (2014b), Comparative geochemistry of rhenium in oxidized arc magmas and MORB and rhenium partitioning during magmatic differentiation, *Chem. Geol.*, *386*, 101–114, doi:10.1016/j.chemgeo.2014.08.013.

Li, Y., and A. Audétat (2012), Partitioning of V, Mn, Co, Ni, Cu, Zn, As, Mo, Ag, Sn, Sb, W, Au, Pb, and Bi between sulfide phases and hydrous basanite melt at upper mantle conditions, *Earth Planet. Sci. Lett.*, *355–356*, 327–340, doi:10.1016/j.epsl.2012.08.008.

Liu, X., X. Xiong, A. Audétat, Y. Li, M. Song, L. Li, W. Sun and X. Ding (2014), Partitioning of copper between olivine, orthopyroxene, clinopyroxene, spinel, garnet and silicate melts at upper mantle conditions, *Geochim. Cosmochim. Acta*, *125*, 1–22, doi:10.1016/j.gca.2013.09.039.

Mallmann, G., and H. St. C. O'Neill (2009), The crystal/melt partitioning of V during mantle melting as a function of oxygen fugacity compared with some other elements (Al, P, Ca, Sc, Ti, Cr, Fe, Ga, Y, Zr and Nb), *J. Petrol.*, *50*(9), 1765–1794, doi:10.1093/petrology/egp053.

Massoth, G., et al. (2007), Multiple hydrothermal sources along the south Tonga arc and Valu Fa Ridge, *Geochem. Geophys. Geosyst.*, *8*, Q11008, doi:10.1029/2007GC001675.

Mathez, E. A. (1976), Sulfur solubility and magmatic sulphides in submarine basalt glass, *J. Geophys. Res.*, *81*(23), 4269–4276, doi:10.1029/JB081i023p04269.

Mavrogenes, J. A., and H. St. C. O'Neill (1999), The relative effects of pressure, temperature and oxygen fugacity on the solubility of sulfide in mafic magmas, *Geochim. Cosmochim. Acta*, *63*(7–8), 1173–1180, doi:10.1016/S0016-7037(98)00289-0.

Melekhova, E., C. Annen, and J. Blundy (2013), Compositional gaps in igneous rock suites controlled by magma system heat and water content, *Nat. Geosci.*, *6*(5), 385–390, doi:10.1038/ngeo1781.

Metrich, N., A. J. Berry, H. St. C. O'Neill, and J. Susini (2009), The oxidation state of sulfur in synthetic and natural glasses determined by X-ray absorption spectroscopy, *Geochim. Cosmochim. Acta*, *73*, 2382–2399, doi:10.1016/j.gca.2009.01.025.

Michael, P. (1995), Regionally distinctive sources of depleted MORB: Evidence from trace elements and H_2O, *Earth Planet. Sci. Lett.*, *131*(3–4), 301–320, doi:10.1016/0012-821X(95)00023-6.

Mikkelson, N. (2005), *The Major Element Geochemistry and Oxidation States of Back Arc Basins in the South West Pacific*, 83 pp., Aust. Natl. Univ., Canberra.

Moore, J. (1970), Water content of basalt erupted on the ocean floor, *Contrib. Mineral. Petrol.*, *28*(4), 272–279, doi:10.1007/BF00388949.

Moss, R., and S. D. Scott (2001), Gold content of eastern Manus basin volcanic rocks: Implications for enrichment in associated hydrothermal precipitates, *Econ. Geol.*, *96*, 91–107, doi:10.2113/gsecongeo.96.1.91.

Mungall, J. (2002), Roasting the mantle: Slab melting and the genesis of major Au and Au-rich Cu deposits, *Geology*, *30*, 915–918, doi:10.1130/0091-7613(2002).

Newman, S., and J. B. Lowenstern (2002), VolatileCalc: A silicate melt-H_2O-CO_2 solution model written in Visual Basic for excel, *Comput. Geosci.*, *28*(5), 597–604, doi:10.1016/s0098-3004(01)00081-4.

O'Neill, H. St. C., and F. E. Jenner (2012), The global pattern of trace-element distributions in ocean floor basalts, *Nature*, *491*, 698–704, doi:10.1038/nature11678.

O'Neill, H. St. C., D. B. Dingwell, A. Borisov, B. Spettel, and H. Palme (1995), Experimental petrochemistry of some highly siderophile elements at high temperatures, and some implications for core formation and the mantle's early history, *Chem. Geol.*, *120*(3–4), 255–273, doi:10.1016/0009-2541(94)00141-T.

Palme, H., and H. St. C. O'Neill (2014), Compositional estimates of mantle composition, in *The Mantle and Core*, edited by R. W. Carlson, Elsevier, Oxford, U. K.

Park, J.-W., I. H. Campbell, and R. J. Arculus (2013), Platinum-alloy and sulfur saturation in an arc-related basalt to rhyolite suite: Evidence from Pual Ridge, Eastern Manus Basin, *Geochim. Cosmochim. Acta*, *101*, 76–95, doi:10.1016/j.gca.2012.10.001.

Park, J.-W., I. H. Campbell, J. Kim, and J.-W. Moon (2015), The role of late sulfide saturation in the formation of a Cu- and Au-rich magma: Insights from the platinum group element geochemistry of Niuatahi-Motutahi lavas, Tonga Rear Arc, *J. Petrol.*, *56*(1), 59–81, doi:10.1093/petrology/egu071.

Patten, C., S.-J. Barnes, E. A. Mathez, and F. E. Jenner (2013), Partition coefficients of chalcophile elements between sulfide and silicate melts and the early crystallization history of sulfide liquid: LA-ICP-MS analysis of MORB sulfide droplets, *Chem. Geol.*, *358*, 170–188, doi:10.1016/j.chemgeo.2013.08.040.

Pearce, J. A., R. C. Stern, S. H. Bloomer, and P. Fryer (2005), Geochemical mapping of the Mariana arc-basin system: Implications for the nature and distribution of subduction components, *Geochem. Geophys. Geosyst.*, *6*, Q07006, doi:10.1029/2004GC000895.

Plank, T., K. A. Kelley, M. M. Zimmer, E. H. Hauri, and P. J. Wallace (2013), Why do mafic arc magmas contain ~4 wt % water on average?, *Earth Planet. Sci. Lett.*, *364*, 168–179, doi:10.1016/j.epsl.2012.11.044.

Richards, J. P. (2003), Tectono-magmatic precursors for porphyry Cu-(Mo-Au) deposit formation, *Econ. Geol.*, *98*(8), 1515–1533, doi:10.2113/gsecongeo.98.8.1515.

Richards, J. P. (2011), Magmatic to hydrothermal metal fluxes in convergent and collided margins, *Ore Geol. Rev.*, *40*(1), 1–26, doi:10.1016/j.oregeorev.2011.05.006.

Righter, K., W. P. Leeman, and R. L. Hervig (2006), Partitioning of Ni, Co and V between spinel-structured oxides and silicate melts: Importance of spinel composition, *Chem. Geol.*, *227*, 1–25, doi:10.1016/j.chemgeo.2005.05.011.

Sillitoe, R. H. (2010), Porphyry copper systems, *Econ. Geol.*, *105*(1), 3–41, doi:10.2113/gsecongeo.105.1.3.

Simon, A. C., P. A. Candela, P. M. Piccoli, M. Mengason, and L. Englander (2008), The effect of crystal-melt partitioning on the budgets of Cu, Au, and Ag, *Am. Mineral.*, *93*(8–9), 1437–1448, doi:10.2138/am.2008.2812.

Sisson, T. W., and T. L. Grove (1993), Experimental investigations of the role of H_2O in calc-alkaline differentiation and subduction zone magmatism, *Contrib. Mineral. Petrol.*, *113*(2), 143–166, doi:10.1007/BF00283225.

Sun, W., R. J. Arculus, V. S. Kamenetsky, and R. A. Binns (2004), Release of gold-bearing fluids in convergent margin magmas prompted by magnetite crystallization, *Nature*, *431*, 975–978, doi:10.1038/nature02972.

Sun, W., et al. (2015), Porphyry deposits and oxidized magmas, *Ore Geol. Rev.*, *65*(Part 1), 97–131, doi:10.1016/j.oregeorev.2014.09.004.

Tan, J., J. Wei, A. Audétat, and T. Pettke (2012), Source of metals in the Guocheng gold deposit, Jiaodong Peninsula, North China Craton: Link to early Cretaceous mafic magmatism originating from Paleoproterozoic metasomatized lithospheric mantle, *Ore Geol. Rev.*, *48*, 70–87, doi:10.1016/j.oregeorev.2012.02.008.

Timm, C., C. E. J. de Ronde, M. I. Leybourne, D. Layton-Matthews, and I. J. Graham (2012), Sources of chalcophile and siderophile elements in Kermadec arc lavas, *Econ. Geol.*, *107*(8), 1527–1538, doi:10.2113/econgeo.107.8.1527.

Toplis, M., and A. Corgne (2002), An experimental study of element partitioning between magnetite, clinopyroxene and iron-bearing silicate liquids with particular emphasis on vanadium, *Contrib. Mineral. Petrol.*, *144*(1), 22–37, doi:10.1007/s00410-002-0382-5.

Tuff, J., and H. St. C. O'Neill (2010), The effect of sulfur on the partitioning of Ni and other first-row transition elements between olivine and silicate melt, *Geochim. Cosmochim. Acta*, *74*(21), 6180–6205, doi:10.1016/j.gca.2010.08.014.

Vallier, T. L., et al. (1991), Subalkaline andesite from Valu Fa Ridge, a back-arc spreading center in southern Lau Basin: Petrogenesis, comparative chemistry, and tectonic implications, *Chem. Geol.*, *91*(3), 227–256, doi:10.1016/0009-2541(91)90002-9.

Wilkinson, J. J. (2013), Triggers for the formation of porphyry ore deposits in magmatic arcs, *Nat. Geosci.*, *6*, 917–925, doi:10.1038/ngeo1940.

Wohlgemuth-Ueberwasser, C., R. C. Fonseca, C. Ballhaus, and J. Berndt (2012), Sulfide oxidation as a process for the formation of copper-rich magmatic sulfides, *Miner. Deposita*, *48*, 115–127, doi:10.1007/s00126-012-0420-9.

Wood, S. A. (1987), Thermodynamic calculations of the volatility of the platinum group elements (PGE): The PGE content of fluids at magmatic temperatures, *Geochim. Cosmochim. Acta*, *51*(11), 3041–3050, doi:10.1016/0016-7037(87)90377-2.

Wykes, J. L., H. St. C. O'Neill, and J. A. Mavrogenes (2010), The effect of FeO on the sulfur content at sulfide saturation (SCSS): A comparison between sulfur and selenium, in *11th International Platinum Symposium*, Ontario Geological Survey, Miscellaneous Release–Data 269.

Zajacz, Z., P. A. Candela, P. M. Piccoli, and C. Sanchez-Valle (2012), The partitioning of sulfur and chlorine between andesite melts and magmatic volatiles and the exchange coefficients of major cations, *Geochim. Cosmochim. Acta*, *89*, 81–101, doi:10.1016/j.gca.2012.04.039.

Zajacz, Z., P. A. Candela, P. M. Piccoli, C. Sanchez-Valle, and M. Wälle (2013), Solubility and partitioning behavior of Au, Cu, Ag and reduced S in magmas, *Geochim. Cosmochim. Acta*, *112*, 288–304, doi:10.1016/j.gca.2013.02.026.

Zelenski, M., N. Malik, and Y. Taran (2014), Emissions of trace elements during the 2012–2013 effusive eruption of Tolbachik volcano, Kamchatka: Enrichment factors, partition coefficients and aerosol contribution, *J. Volcanol. Geotherm. Res.*, *285*, 136–149, doi:10.1016/j.jvolgeores.2014.08.007.

Zimmer, M. M., T. Plank, E. H. Hauri, G. M. Yogodzinski, P. Stelling, J. Larsen, B. Singer, B. Jicha, C. Mandeville, and C. J. Nye (2010), The role of water in generating the calc-alkaline trend: New volatile data for aleutian magmas and a new tholeiitic index, *J. Petrol.*, *51*(12), 2411–2444, doi:10.1093/petrology/egq062.